In Situ TEM Electromechanical Testing of Nanowires and Nanotubes

Horacio D. Espinosa, Rodrigo A. Bernal, and Tobin Filleter*

Material published in this Review will also appear in *Nano and Cell Mechanics: Fundamentals and Frontiers* by John Wiley & Sons, Ltd.

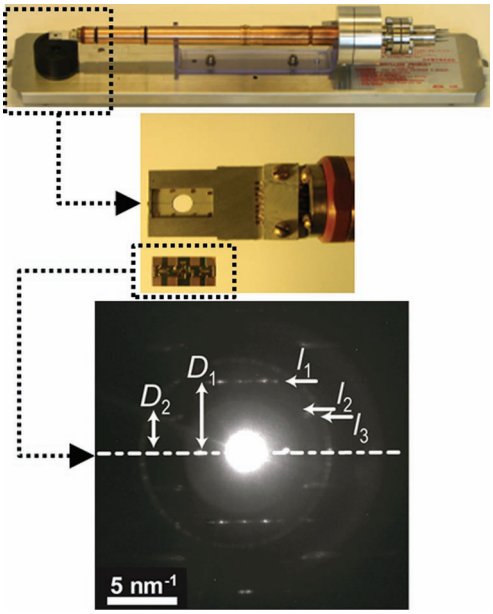

From the Contents

The emergence of one-dimensional nanostructures as fundamental constituents of advanced materials and next-generation electronic and electromechanical devices has increased the need for their atomic-scale characterization. Given its spatial and temporal resolution, coupled with analytical capabilities, transmission electron microscopy (TEM) has been the technique of choice in performing atomic structure and defect characterization. A number of approaches have been recently developed to combine these capabilities with in-situ mechanical deformation and electrical characterization in the emerging field of in-situ TEM electromechanical testing. This has enabled researchers to establish unambiguous synthesis-structure-property relations for one-dimensional nanostructures. In this article, the development and latest advances of several in-situ TEM techniques to carry out mechanical and electromechanical testing of nanowires and nanotubes are reviewed. Through discussion of specific examples, it is shown how the merging of several microsystems and TEM has led to significant insights into the behavior of nanowires and nanotubes, underscoring the significant role in-situ techniques play in the development of novel nanoscale systems and materials.

1. Introduction

One-dimensional nanostructures, namely nanowires and nanotubes, have emerged as feasible building blocks for the next generation of devices and materials, with applications envisioned in electronics, sensors, and energy technologies. Nanotubes, long used as test beds of fundamental phenomena, are now viable alternatives for electronic systems[1] and are used as the fundamental constituent of high performance fibers,[2] given their outstanding mechanical[3] and transport properties.[4] On the other hand, semiconducting and metallic nanowires are envisioned as interconnects in next generation electronics,[5] building blocks of nanophotonic systems,[6] and energy conversion elements for self-powered nanodevices.[7]

The wide technological applicability of nanowires and nanotubes has elicited demand for their extensive characterization. Such characterization is critical in order to quantify their mechanical, electrical, thermal, chemical and physical properties, and generate data that can be used at the design and manufacturing stage to optimize synthesis, device architecture and performance.

From the different types of characterization that can be carried-out, measurement of mechanical and electromechanical properties are of high relevance to most applications. These measurements provide parameters for operation of devices that require mechanical movement to achieve functionality, and more importantly, offer insight into failure limits and associated mechanisms in nanostructures. In turn, this provides much needed data towards reliable and robust designs, which are critical if nanostructures are to find widespread usage in future consumer applications.[8]

The characterization of mechanical and electromechanical properties of one-dimensional nanostructures is becoming a mature field in which numerous researchers pursue characterization using a vast array of techniques. However, this undertaking continues to prove challenging for two main reasons. The first is the characteristic size of the specimen under study (e.g., diameter), which ranges from a few nanometers to up to several hundred nanometers. This renders specimen manipulation and preparation for testing very difficult, and it imposes highly demanding requirements in metrology and instrumentation. The second is the diverse variety of one-dimensional nanostructures and their marked structural dependence on synthesis methods. For instance, for carbon nanotubes, the chirality and diameter, which control many properties, have not yet been controlled during growth, and only post-growth sorting methods allow the obtention of monodisperse solutions of nanotubes.[9] For nanowires, although diameter and structural control is fairly good,[10] dopant concentrations may be nonuniform,[11] systematic defects such as stacking faults are possible,[12] and incorporated impurities during growth can be present,[13] among other complications. As a result, it is difficult to propose a universal technique or testing method that is suitable for every nanostructure, as sample preparation and testing will require tailoring to the specific nanomaterial to varying degrees. More importantly, the possible presence of non-uniform defects or impurities, even in nanostructures of the same material, imposes the need to thoroughly characterize the very same nanostructure that is mechanically or electromechanically tested in order to establish unambiguous synthesis-structure-property relations for a given nanomaterial.

In this article, we review the mechanical and electromechanical testing of one-dimensional nanostructures carried out *in situ* transmission electron microscopes (TEM). It will be argued that given the aforementioned constraints for establishing structure-property-relations for these specimens, in situ TEM testing is a technique that excels at enhancing our understanding of 1D nanostructures. The article presents a critical review of the available experimental techniques and several examples that showcase the capabilities of in situ TEM to uncover new phenomena in several nanomaterials. Throughout this review, it will be argued that given the challenges in mechanical and electromechanical characterization of nanostructures, the extremely high atomic resolution achieved in the TEM in addition to its analytical capabilities make *in situ* TEM one of the most suitable techniques for carrying out such measurements.[141]

2. Background

2.1. Relevance of Mechanical and Electromechanical Testing for One-Dimensional Nanostructures

As mentioned above, one-dimensional nanostructures have emerged as viable alternatives for new materials and devices. For instance, carbon nanotubes (CNTs) are being used to develop novel yarns[2] with specific energy to failure similar to that established for spider silk but with higher specific strengths.[2] Still, yarn strength is much lower than that of pristine CNTs (1 TPa modulus and 100 GPa strength[3]). Hence, mechanical testing of CNTs, CNT bundles and their interaction, with atomic resolution, presents a unique opportunity for multiscale design of materials with properties scaled to the macroscale.[17] In the case of other nanomaterials such as semiconducting and metallic nanowires, with applications in electronics, plasmonics and photonics, mechanical and electromechanical properties are of relevance, although a direct link sometimes may not be explicit. However, there are several examples in which these properties are at the core of establishing the behavior of nanoscale materials and devices. Take for example the case of nanogenerators engineered with semiconducting, piezoelectric

Prof. H. D. Espinosa, R. A. Bernal, Prof. T. Filleter[+]
Department of Mechanical Engineering
Northwestern University
2145 Sheridan Rd., Evanston, IL 60208-3111, USA
E-mail: espinosa@northwestern.edu
[+] Present address: Department of Mechanical and Industrial Engineering, University of Toronto, Toronto, ON M5S 3G8, Canada

DOI: 10.1002/smll.201200342

small

nanowires[18] and strips or fibers of piezoelectric materials such as Lead-Zirconate-Titanate (PZT).[19] These devices produce electrical energy, which is envisioned to power personal electronic devices, by harvesting mechanical energy coming from, for example, body motions or vibrations, and converting it to electricity via the piezoelectric effect. In the case of semiconducting nanowires, mechanical and piezoelectric properties of ZnO nanowires were necessary to establish the amount of voltage produced by the nanogenerating scheme.[20] Charges were estimated by using a mathematical model that linked the elastic, piezoelectric and dielectric properties of the material, as well as its carrier concentration. In the case of PZT nanoribons, the mechanical properties were necessary for designing a device that can buckle and stretch the fibers to generate electricity without undergoing fracture.[21]

Another example where the knowledge of mechanical and electromechanical properties has proven important is in the investigation of piezoresistance in silicon nanowires. In order to extract the piezoresistive coefficient and decouple the changes in resistance from dimensional changes, knowledge of stresses and strains in the nanowire is necessary. In a highly cited paper where giant piezoresistance in silicon nanowires was demonstrated,[22] calculations were performed using the values of bulk silicon. However, it has been found that depending on the orientation, the modulus of silicon nanowires changes as their dimensions decrease.[23] This points to the need for measuring all nanowire properties during electromechanical tests. Given that size-dependent elastic behavior[24] and surface states that induce electron and hole trapping[25] were not considered in the initial report, giant piezoresistance continuous to be a subject of debate. One can also cite the usage of silicon nanowires for lithium batteries, where knowledge of their mechanical properties and theoretical modeling of the deformation processes during lithiation are fundamental to understand why the nanowires withstand the extreme volume changes that make them good electrode materials.[26]

Finally, we point out that knowledge of deformation and mechanical properties are of relevance to other nanostructures, for example, nanoparticles. In such case, surface steps are known to influence catalytic and thermal properties, while knowledge of their mechanical properties is critical when they are incorporated into polymeric nanocomposites.[27] There is also increased scientific interest in dislocation mechanisms in nanoparticles since several experiments have indicated absence of dislocation at large strains, or their disappearance upon unloading.[27,28]

The previous examples showcase that knowledge of mechanical and electromechanical properties is paramount to understand and optimize the behavior of nanostructured materials and nanoscale devices. Hence, characterization of mechanical properties in one-dimensional nanomaterials has played, and will continue to play an important role in addressing challenges of reliability, robustness and functionality of systems with nanoscale architectures. Having established that mechanical property characterization is an important field of study, we next discuss one of the most accurate and powerful techniques for doing so.

Horacio Espinosa is the chair and director of the Theoretical and Applied Mechanics program, and a Professor in the Department of Mechanical Engineering at Northwestern University. He received his PhD degree from Brown University in 1992. Prof. Espinosa has made contributions in the areas of dynamic failure of advanced materials, computational modeling of fracture, and multiscale experiments and simulations of micro- and nanosystems. He has published over 200 technical papers in these fields.

Rodrigo Bernal is a PhD student in the department of Mechanical Engineering at Northwestern University. He received a bachelor's degree in Mechanical and Electronics Engineering from Los Andes University in Bogotá, Colombia. His undergraduate work focused on powder metallurgy and development of low-cost Scanning Probe Microscopes. He joined Prof. Espinosa's lab in the fall of 2008. His current research interests include the mechanical and piezoelectric properties of semiconducting nanowires, in-situ testing of nanostructures and nanomanipulation.

Tobin Filleter is currently an Assistant Professor in the Department of Mechanical and Industrial Engineering at the University of Toronto. Previously, he was a postdoctoral fellow in the Department of Mechanical Engineering at Northwestern University. He received a bachelor's degree in Engineering Physics from Queen's University in 2003 and a PhD in Physics from McGill University in 2009. His research interests include nanotribology and atomic-scale friction, in-situ SEM/TEM mechanical testing, multiscale experiments of nano-systems, and the mechanics of graphene and CNTs.

2.2. Mechanical and Electromechanical Characterization of Nanostructures: The Need for In situ TEM

There are several requirements for carrying out accurate mechanical and electromechanical characterization at the nanoscale. These are:

1. Precise measurements of forces and displacements/strains. We highlight the fact that it is much preferred for both to be measured as otherwise an assumption of constitutive behavior — which is not always available for nanoscale materials — has to be made.
2. Precise measurement of the specimen cross-sectional area. This is important for calculating stress from the measurement of force.[29] Given the dimension of nanoscale specimens, resolution is important and errors in measurement of the cross-sectional area become more important as size decreases.

3. Knowledge of preexisting defects, crystalline and surface quality of the specimen.
4. In the case of electromechanical measurements, adequate resolution of the electrical variables (current and voltage).
5. Real-time or near real-time observation of the experiment in order to establish cause-effect relations, metastable states, and mechanisms of fracture or failure.[30,31]

The measurement of force and electrical quantities is typically more dependent on the particular setup used to deform the nanostructure. Depending on the employed sensor, the measurement of force may not depend on spatial input but rather on other electrical variables such as electronic noise. In the same vein, the measurement of electrical quantities depends primarily on the instrumentation available, and in the establishment of proper electrical contacts to the nanostructure (Ohmic or Schottky, depending on the desired measurement).

On the other hand, the measurement of strains, displacements and cross-sectional areas, and the identification of defects depend directly on the temporal and spatial resolution of the instrument where the mechanical deformation is visualized. Given the dimensions of nanostructures, optical microscopes are mostly inadequate, narrowing the possible choices to electron microscopy and scanning probe microscopy (the latter with some limitations as explained below). Within electron microscopy, conventional TEM, and aberration-corrected TEM have nanometer and sub-angstrom resolution,[32] respectively, which is much superior to conventional scanning-electron microscopy (SEM). Additionally, an array of analytical capabilities (with a probe size on the nanometer scale) complement resolution, providing information about crystalline quality, preexisting defects and chemical composition.[14,33]

Temporal resolution is another advantage of TEM, as it usually can capture images at TV rate (~30 frames-per-second).[34] This makes it superior for real time in situ testing over similar-resolution techniques such as Scanning Tunneling Microscopy (STM) or other scanning probe techniques (atomic force microscopy, AFM), where slow scanning is often required to achieve ultimate resolution. Thus, the TEM is able to resolve a given area with atomic resolution in a shorter time-span than what it would be possible with scanning probe techniques.

Recent efforts have been made to extend the time resolution of the TEM to the nanosecond (ns) and even femtosecond (fs) regime. This is accomplished by the use of two laser pulses, one triggering changes in the specimen and the other triggering the electron emission necessary to obtain a TEM image. By careful control of the delay between the pulses, resolutions of 15 ns,[35] and even fs[36] have been achieved. In the first case, called Dynamic-TEM (DTEM), the aim is to obtain one complete TEM image per laser shot. However, the large number of electrons needed to form an image in this fashion compromises spatial resolution.[37] In the second case, called four-dimensional ultrafast electron microscopy (4D-UEM),[36] the response of many fs-scale electron pulses is integrated over time in one image (the so-called stroboscopic approach), preserving high spatial resolution.[37] In both cases, a single experiment cannot be followed over time, given the impossibility of capturing images at fs or ns rates with a CCD (charge coupled device) detector. Instead, several experiments are carried out at varying delay times, capturing an image in each one.[38] Nevertheless, the time scales reached are unprecedented, extending the accessible time scale for TEM to the realm of phase transformations, chemical reactions and even atomic motions.[36] A summary of the advantages of TEM in temporal and spatial resolution are illustrated in **Figure 1**.[33]

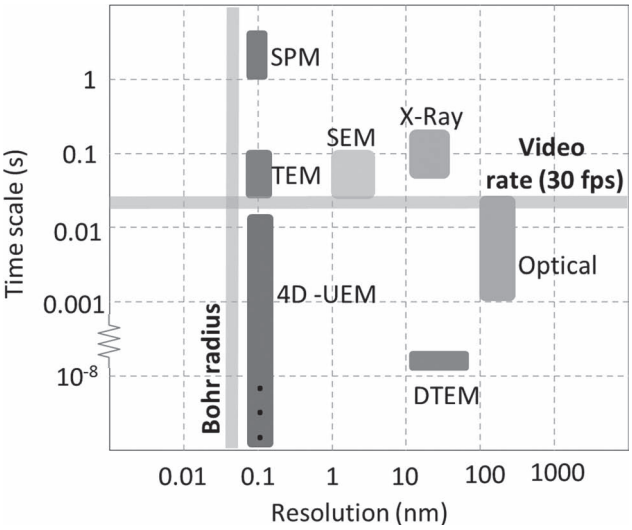

Figure 1. Temporal and spatial resolution of several microscopy techniques. TEM and related techniques (4D-UEM, DTEM) cover the highest spatial and time resolutions. X-ray resolutionfrom Ref,[140] DTEM from,[35,37] and 4D-UEM from.[36]

The identification of preexisting defects in 1D-nanostructures and its relevance to mechanical and electromechanical properties deserves special attention.[39] Crystalline defects such as stacking faults and dislocations are known to influence the mechanical response. However, their influence on electromechanical properties is often overlooked. Inversion domain boundaries, by creating anti-parallel polarizations, and dislocations, by inducing a localized strain field, have an effect on piezoelectricity.[40] On the other hand, the role of stacking faults and surface defects is not well established, although stacking faults locally affect the band structure.[40] All of the aforementioned defects have been identified in nanostructures. More importantly, their identification was achieved exclusively using TEM[12,41–44] which attests to its suitability to evaluate crystalline structure in 1-D nanostructures. Evidently, all the aforementioned advantages of the TEM for structural characterization are not exclusive to nanowires and nanotubes, but to other nanostructures such as nanoparticles.[27]

In conclusion, TEM clearly possesses superior capabilities to thoroughly and unambiguously characterize the mechanical and electromechanical response of one-dimensional nanostructures. In the following sections, we present a survey of the most impactful experimental setups and scientific

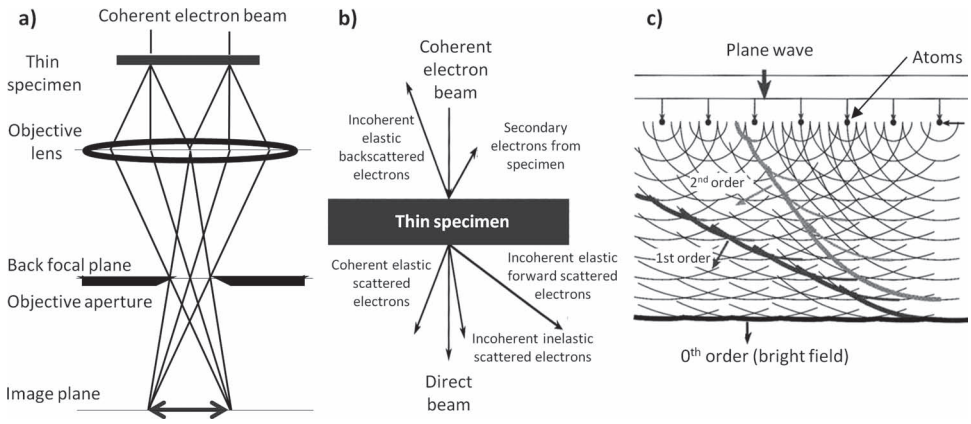

Figure 2. Basic concepts of TEM. a) Simplified schematic of the electron-path inside a TEM column. b) Schematic of the different interactions of the incident electrons with the electrons from the specimen. These interactions are useful in several analytical techniques in the TEM. c) Schematic of the formation of diffraction spots. The structure and periodicity of the diffraction pattern is directly related to the structure and periodicity of the atoms in the specimen. Figures b,c) adapted with kind permission.[14] Copyright 2009, Springer Science and Business Media.

discoveries that demonstrate how TEM has, and will continue to provide unprecedented insight into the fundamental synthesis-structure-properties relations for nanostructures.

3. In-Situ TEM Experimental Methods

In the previous section, it was established that in situ TEM is the technique-of-choice to carry out mechanical and electromechanical characterization of nanoscale specimens. Here we will provide a short summary of the basic principles of TEM, followed by a review of the different experimental setups that have been developed to carry out testing inside the TEM as well as the specimen preparation techniques used for positioning one-dimensional nanostructures in the testing setups.

The TEM operates by passing a mostly coherent (temporal and spatial coherence lengths are in the order of a few hundred and a few nanometers, respectively[14]) beam of electrons through a thin specimen. Given the wavelength of the electrons, the potential resolution is well below the size of an atom.[14] Indeed, recent advances in aberration-corrected TEMs have allowed resolutions of 80 pm.[32] The electron beam is focused through a series of electron-lenses after passing through the sample, and finally impinges an electroluminescent screen or CCD detector that provides a visible output related to the image created by the electrons passing through the sample. Movies may be recorded by continuously acquiring images from the CCD. A simplified schematic of this concept is shown in **Figure 2**a.

Given that the high energy electrons (~50–200 keV in conventional TEMs) are ionizing radiation, some electrons from the sample can interact with the beam, causing scattering of electrons, which in turn provides information about the specimen structure and composition.[14] Many of the analytical techniques in the TEM that allow elemental or other types of characterization are based on these scattered electrons. On the other hand, electrons that passed unscattered through the sample (the direct beam) are used to form the so-called bright–field image, which, for most practical applications, represents the projection of the sample along the direction of the beam. A schematic of this is shown in Figure 2b.

Electron diffraction is also a very useful feature of the TEM. The diffracted beams (Figure 2c) are directly correlated to the atomic structure of the sample. Thus, electron diffraction in the TEM can be used to identify crystalline structure and to obtain, among several measurements, interplanar spacing, useful for measuring strains in the specimen.

Of particular relevance to the investigation of 1D nanostructures is the TEM capability of performing analytical studies, diffraction and imaging in the scale of a few-nanometers or even atomic-scale, which enables thorough characterization of the nanospecimen and may uncover localized phenomena such as amorphization, created by large inhomogenous strains.[45]

3.1. Overview of TEM Specimen Holders

One of the challenges of carrying out *in situ* testing in the TEM arises because the functional part of the experimental setup must fit within the limited volume available in TEMs for the specimen holder. The thickness, which is controlled by the gap between the pole pieces of the lenses, is one of the most stringent dimensional constraints if complex microsystems are used in the experimental setup. This constraint becomes more prominent as resolution increases in view that higher resolution usually means a smaller gap, the exception being some specialized aberration corrected instruments where the gap can be up to 20 mm.[30] An illustration of the geometrical characteristics of typical TEM specimen holders is given in **Figure 3**.

For carrying out mechanical and electromechanical testing, researchers have engineered several types of holders and experimental techniques to work around these constraints. Although sometimes this may result in compromises in functionality (e.g., only having primary tilt capabilities[34]), technical advances continue to push the boundaries of what can be done inside the microscope, for example

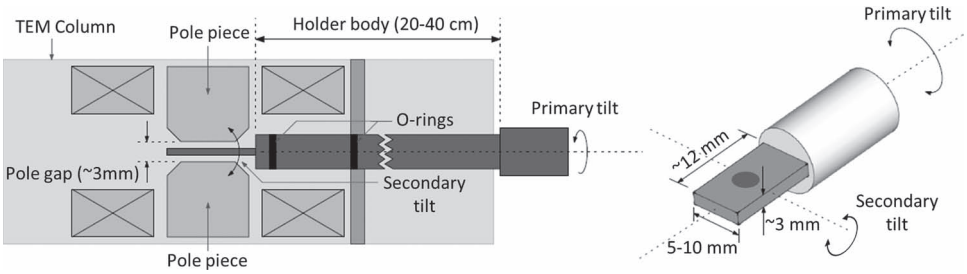

Figure 3. Schematic of a typical TEM specimen holder. Left: Cross-section of a TEM Column and the position of the holder. Right: Perspective view of the holder-tip. The specimen typically has to be within a circle of 3mm diameter (dark grey area). These dimensional constraints result in a limited size for the experimental setup.

microelectromechanical systems (MEMS) that miniaturize the setup so that the size of movable parts is no longer a major concern. In the following section, we discuss several methods and setups for mechanical and electromechanical testing and their application to the testing of one dimensional nanostructures. In each method we present the physical principles that govern the particular measurement technique and the essential technical details of how the method is implemented. We also provide representative results obtained with each technique to illustrate the capabilities of in-situ TEM testing to the mechanical and electromechanical characterization of 1D nanostructures.

3.2. Methods for Mechanical and Electromechanical Testing of Nanowires and Nanotubes

3.2.1. Resonance

Resonance methods deserve a special mention given their historical importance and simplicity. Using this method, the first reports on the experimental measurement of the modulus of CNTs were published.[46,47] Given the success of measuring CNT properties and its relative simplicity, the technique gained quick acceptance and has been used to characterize the properties of other materials.[48,49]

In the resonance characterization method, the modes of vibration of a freestanding nanostructure are characterized and the mechanical properties are extracted based on continuum and statistical mechanical models. The nanostructure is cantilevered on a substrate and is free to vibrate at the tip. In order to observe the vibration, the nanostructure axis must be perpendicular to the axis of the electron-beam and any misalignment must be prevented, using the microscope focus as a guide.[46]

The resonance of the structure can either be thermal or electrostatic. Thermal resonance is observed as blurriness of the tip of the nanostructure and is intrinsic to any system. Electrostatic resonance is induced by the application of an oscillating electric field to the nanostructure.

Thermal resonance has been used to characterize the elastic moduli of carbon[46] and boron nitride nanotubes.[50] A continuum mechanics model of a cylinder, excited by thermal vibrations, is used to relate the geometry, temperature, and modulus to the measured vibration amplitude. The vibration amplitude at the nanostructure-tip as a function of temperature,[46] or as a function of position (keeping the temperature fixed),[50] can be used to extract the elastic modulus.

On the other hand, electrostatic resonance has been used to characterize the elastic moduli of carbon nanotubes,[47] tungsten oxide nanowires,[48] and gallium nitride nanowires.[49] In this method, an oscillating voltage is applied between the specimen and a counter-electrode positioned nearby, which creates an oscillating electric field that in turn induces oscillations in the nanostructure. By sweeping the frequency of the voltage, the resonance frequencies (fundamental or harmonics) of the nanostructure can be identified. The mechanical properties are extracted via a continuum mechanics model that relates the measured resonance frequency, geometry, density and elastic modulus of the material. Note that this method has also been applied in SEM for the characterization of elastic modulus of other nanostructures, such as zinc oxide nanowires.[51]

The resonance method has the advantage of being easily implementable as it does not require a very sophisticated TEM holder (see **Figure 4**a). In addition, sample preparation is relatively straightforward. However, only the measurement of elastic modulus is possible while measurement of stress-strain response and fracture strength and strain is not. The difficulty of precisely identifying the amplitude of thermal vibration has also been pointed out to lead to experimental uncertainties.[47]

3.2.2. TEM/SPM and Nanoindenter-Based Compression, Tension and Bending

Some of the resonance setups that were proposed in early years had, as one of the two electrodes, a small movable tip actuated by a piezoelectric tube scanner, similar to the early setups of scanning tunneling microscopy. This initial idea of having a nanometer-precision movable tip opposing another electrode, all embedded in a TEM specimen holder, has evolved into three main setup types. When these are combined, they account for the majority of reported results of mechanical, electrical and electromechanical tests of nanostructures in situ TEM. These classes are respectively, the nanoindenter setup, the so-called STM/TEM (STM-Scanning-Tunneling-Microscope) and the so-called AFM/TEM (AFM–Atomic Force Microscope). The latter two are often grouped under the name TEM/SPM (SPM—Scanning Probe Microscopy). The common idea in these setups is to utilize

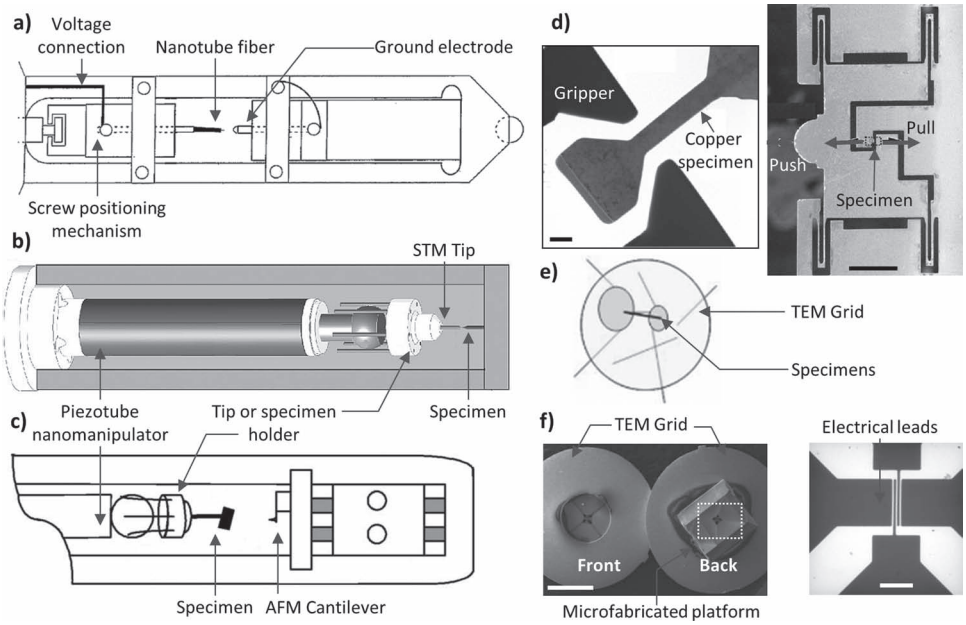

Figure 4. Schematics of some of the different setups available for TEM electro/mechanical characterization. From figures a) to c) the particular TEM holder-tip is shown. a) Holder-tip for the electrostatic resonance method. Note the two terminals used to introduce an AC electrostatic field to the specimen. Reprinted with permission.[106] Copyright 2000, IUPAC. b) STM/TEM system where a STM head is used to deform the sample and electrical measurements are possible. Reprinted with permission.[64] Copyright 2003, American Institute of Physics. c) An evolution of STM/TEM is the AFM/TEM where a cantilever can be used to measure force, and in selected cases, also apply electrical signals. Reprinted with permission.[80] Copyright 2008, IEEE. d) Nanoindenter-based extensions for 1D nanostructure testing. On the left, a gripper tensions a FIB-fabricated copper specimen. Scale bar: 200 nm. On the right, a microfabricated flexure converts the compressing motion of the indenter to tension. Scale bar: 100 µm. Reprinted with permission.[60,61] Copyright 2011, American Chemical Society. e) TEM grid covered with a collodion thin film that stretches under e-beam irradiation, thus straining the specimens. Reprinted with permission.[45] Copyright 2007, American Chemical Society. f) TEM grid with a microfabricated platform allowing 4-point measurements. The image in the right shows a magnified view of the dashed square on the left. Scale bars: 1 mm, 50 µm. Reprinted with permission.[104] Copyright 2006, IOP Publishing Inc.

the moving tip to deform the sample in some fashion while visualizing it in situ TEM. Depending on the setup, the electrical and mechanical consequences of said deformations can be measured and correlated. Common to all the setups is a predominance of compressive deformations, either homogeneous in the case of pillars, or heterogeneous when slender specimens are compressed and later buckled or bent.

The exception to this is the atom-sized specimens created from contact and retraction of the two electrodes.[52] These three setups will be briefly explained below; for a comprehensive review of nanoindentation setups, see Stach,[53] for STM-AFM/TEM, see Nafari et al.[34]

Nanoindentation and Pillar Compression: The nanoindenter setup was initially implemented using a piezo-tube scanner pushing against the specimen to impose deformation through a diamond tip or punch.[54] Although indentation as a technique to impose deformation is outside the scope of this review, we mention it because this setup has evolved towards the testing of one-dimensional nanostructures and can be considered a precursor of the TEM/STM setup. Nowadays, commercial nanoindenter setups exist and are widely used. They consist of an electrostatic actuator that employs capacitive sensing for the measurement of force.

These setups have been typically used to impose forces in the order of µN[55] to micrometer or submicrometer pillar samples fabricated by focused-ion-beam (FIB) milling. Until very recently, the pillars were in the micron or sub-micron diameter regime and therefore are not one-dimensional nanostructures. However, important developments in the field of size-scale plasticity have been achieved using this setup, in combination with in-situ TEM and SEM experiments. Indeed, it has become clear from experiments in single-crystal metals that the ultimate tensile strength and the yield strength increase with reduction of the specimen size. The exact mechanism of this increase is still a subject of study and in-situ TEM experiments play a critical role given that it is the only technique where dislocation activity (such as nucleation or annihilation at free surfaces) and preexisting defects, both critical to the behavior of the specimen, can be characterized. The results in this field are extensive and beyond the scope of this article, but the reader is referred to[56,57] for recent reviews.

Nowadays, submicrometer experiments in situ TEM and SEM are starting to be carried out.[58] One example where this class of setups has been used for nanostructures is the work by Huang et al.[59] where sub-micron GaN nanowires with very low aspect ratio (in the guise of pillars) were compressed to failure.

An important new development that will likely extend the range of this technique towards submicrometer 1D nanostructures is the development of modified nanoindenter tips and microfabricated stages for tensile testing

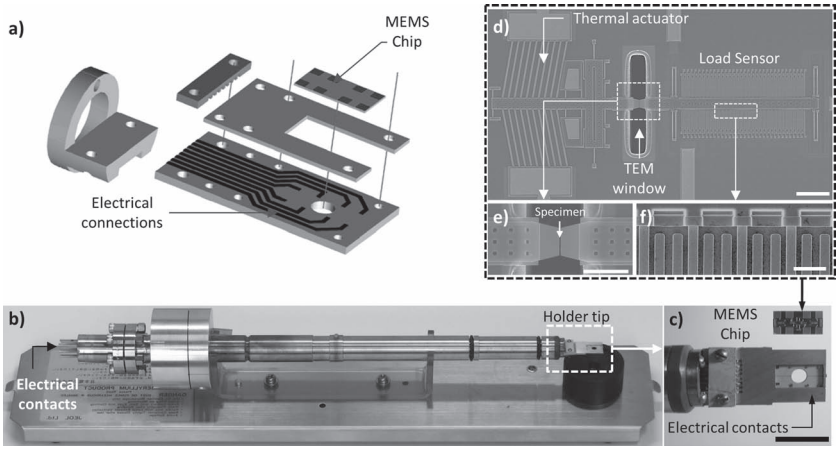

Figure 5. MEMS devices for in situ TEM testing. a) TEM holder Tip showing the interfacing of electrical connections with the terminals of the MEMS chip. Reprinted with permission.[92] Copyright 2005, Cambridge University Press. b,c) TEM holder for the MEMS chip. Scale bar in c) is 10 mm. Reprinted with permission.[88] Copyright 2010, Cambridge University Press. d) SEM micrograph of the MEMS device developed by Espinosa and co-workers. Note the thermal actuator, load sensor and the window allowing observation of the sample in TEM. Scale bar: 100 μm. e) Magnified view of the shuttles where the specimen is positioned. Scale bar: 40 μm. f) Magnified view of the differential capacitors for detecting displacement of the load sensor. Scale bar: 15 μm.

(see **Figure 5**d). In the first case, dog-bone specimens with dimensions in the 100–200 nm diameter regime, fabricated by FIB, are pulled by a nanoindenter tip in the shape of a gripper. This setup was employed in copper specimens to prove that in the submicron regimes, dislocation sourcing and exhaustion influence simultaneously the hardening behavior in metallic specimens.[60] In the second case, a microfabricated flexure was used to convert the compressing motion of the nanoindenter into tension. With this implementation, a 270 nm vanadium dioxide (VO_2) nanowire was strained to achieve phase transformation. The Young's moduli of both M1 and M2 phases in VO_2 was measured (128 ± 10 and 156 ± 10 GPa).[61] It must be pointed out that given the resolution of the nanoindenter setup (sub-μN[55]), tests of smaller-diameter samples, as achieved by other techniques, will require the development of load sensors with greater resolution.

TEM/STM: Using TEM/STM, several interesting phenomena have been probed, such as superplasticity in CNTs,[62] wall by wall current-induced breakdown of multi-walled CNTs (MWCNTs),[63] and the first report on quantized conductance through rows of individual atoms of gold.[52] These are very relevant examples of the employment of high-resolution TEM (HRTEM) to discover new nanoscale phenomena.

The TEM/STM setup consists of two opposing electrodes in the frame of the TEM specimen holder. One of them is fixed and the other is moved by a piezoelectric setup that can operate in fine, and in some cases, coarse motion-regimes, the latter enabled by an inertial mechanism.[64] Depending on the type of experiment, the specimen can be positioned in either electrode and the deformation is imposed by the movement of the movable electrode. In most cases, a tip is positioned in the movable electrode in order to be able to target individual nanostructures. An example of the experimental setup is shown in Figure 4b.

The initial motivation for the development of a TEM/STM setup was to observe the nature of the contact between tip and surface in STM experiments.[65] This continued to be an active area of research, with recent demonstrations of atomic-resolutions scans performed in this type of instrument.[64] However, nowadays this technique is rarely used in the traditional sense of an STM experiment,[34] where the tip performs a raster scan. Rather, the movement of the tip is used to introduce deformations in the nanostructure under study while the electrical properties (current vs. voltage relation) are measured using the electrical capabilities provided by the STM tip. Incidentally, this type of setup has also been used for studying friction of surfaces in-situ the TEM.[66]

One of the limitations of this setup is the lack of measurement of force. As a result, the experiments are limited to correlating the observed deformations with changes in electrical properties, but knowledge of the forces is non-existent or estimated from the strain state. The most usual type of test is the compression and posterior bending, buckling, and fracture of a nanowire or nanotube and the high-resolution observation of the process.[67,68] Nevertheless, given its relative simplicity, STM/TEM continues to be used, accounting for a large portion of the literature on in situ TEM testing of nanostructures.

TEM/AFM: Following the developments of STM/TEM and nanoindenters in situ TEM, more sophisticated setups have been proposed. In particular, instead of just a simple electrode opposing the nanomanipulator, one can position an AFM cantilever, which serves as a force sensor. In this way, mechanical measurements with nN force resolution are possible. Additionally, if the AFM cantilever is conductive and connected to an electrode, coupled electrical and mechanical measurements are possible. An example of the experimental setup is shown in Figure 4c.

With this implementation, kinking of CNTs was observed, where a yield strength of 1.7 GPa was measured.[69] Furthermore, atom-sized specimens, obtained by pulling apart a substrate and an AFM tip coated with the same material have been created. In particular, Au, Cu, and Pd point contacts[70–72] and silicon nanowires[73,74] have been tested. Additional mechanical measurements have been carried out, including filled carbon nanotubes[68,75–77] and ZnO nanowires.[78] In the first studies the difference in mechanical properties between filled and empty nanotubes was established, as well as several mechanisms of failure such as kinking. In the latter study, a elasticity size effect in nanowires previously reported by Agrawal et al. in situ-TEM[79] was observed; additionally, amorphization of the nanowires under repeated bending loads was demonstrated using high resolution imaging and diffraction.

There are three main sub-classes of this type of holder, differentiated by the method utilized to measure the force,

small

i.e., the deflection of the AFM cantilever. In the first case, the deflection is simply measured from images obtained in the bright field mode. In the second case, the laser optical lever system used in traditional AFMs is implemented inside the TEM. In the third case, a piezoresistive cantilever is used to electronically sense the deformation.

Direct imaging of the cantilever has the advantage of simplicity, but it can compromise resolution and accuracy because relatively low magnifications are required if the whole cantilever is imaged. One can use high resolution and image just the contact zone and measure the cantilever deflection based on the displacement of the AFM tip, but this assumes that the field-of-view of the TEM does not drift, which is not always the case. Furthermore, time resolution is limited to the rate of images captured, thus presenting a compromise: the faster the images are captured, the better the time resolution is but the image quality decreases. This is a problem if atomic resolution is needed.

On the other hand, implementing an optical laser system to detect the cantilever deflection is very challenging, but it provides considerable advantages in terms of force and time resolution. This setup has been implemented by Kizuka et al.[70] They used one of the goniometer ports of the TEM to implement the optical setup necessary for detecting the motion of the AFM cantilever. The advantage of this system compared to the previous one is the possibility of obtaining real-time measurements of force with sub-nN resolution. A remarkable example of the advantages of real-time, high resolution measurements of force is the synthesis of stable, high aspect ratio, atomic-scale-width silicon nanowires by withdrawing a point contact, which required continued monitoring and adjusting of the pulling force in order to obtain a stable structure.[74] Coupled mechanical and electrical measurements and atomic-resolution imaging of this specimen were performed, establishing that these atom-sized nanowires can withstand 10^9 to 10^{11} A/m^2 of current density.

Finally, implementing a piezoresistive sensing of the cantilever deflection provides a compromise between the two aforementioned approaches; force resolution is lower, on the order of 15 nN[80] but real time measurement of force is possible. One possible caveat is the drift induced in the sensors by irradiation of the TEM beam.[80] Additionally, custom microfabrication is required to deposit a piezoresistive film over the cantilever and interface it with the setup.

3.2.3. MEMS-Based Testing

MEMS have emerged as the most advanced alternative to create test setups for the mechanical and electrical characterization of nanostructures and other specimens. The use of traditional microfabrication techniques allows the creation of diverse geometries for mechanical testing in a very precise way, which is beneficial for creating tests with carefully controlled boundary conditions. By combining electronically-controlled actuation and sensing, these devices have significant advantages as they apply and measure load and strain independently, while simultaneously allowing for uninterrupted observation of the specimen in HRTEM.[81]

Several nanomaterials have been tested with these devices. In particular, size effects in the elastic and fracture behavior of ZnO and GaN nanowires,[29,79,82] irradiation improvements in the mechanical properties of CNT and CNT-based materials[3,83] and plasticity in penta-twinned silver nanowires[84] have been investigated.

The precursor of the aforementioned MEMS systems for mechanical testing were developed by Haque and Saif.[85] These devices were not strictly MEMS since electronic sensing and actuation were not implemented. Instead, microfabricated flexures were adapted to be actuated by traditional TEM straining holders.[86] These devices allowed measurement of strain by TEM observation but the measurement of force required tracking the movement of a structure with known stiffness. This tracking was achieved by TEM observation as well, which implies that the beam needed to be shifted from the specimen. Moreover, these devices have been mostly used to test thin films or micrometer-sized samples.[87,88]

A MEMS device for nanostructure testing, combining electronic sensing and actuation, was developed by Espinosa and coworkers.[81,88–91] The complete setup for in situ TEM testing using this MEMS device is shown in Figure 5. A custom TEM holder (Figure 5a-c) allows positioning of the MEMS chip inside the TEM and electrical addressing of the electronics for sensing and actuation.[88,92] Figure 5a shows a detailed view of the holder-tip, where it can be seen how the device chip fits in the holder and the way electrical connections are achieved. These connections are then routed outside the TEM by contacts running inside the holder and through a flange (Figure 5b).

The MEMS devices have a thermal actuator and a capacitive load sensor (Figure 5d). The specimen is located in between these two (Figure 5e) and is positioned in the device using a nanomanipulator. Determination of the specimen strain is achieved by direct observation in TEM, either in bright field or in diffraction mode. For force measurement, the displacement of a previously-calibrated load sensor is measured using a set of differential capacitors (Figure 5f).

Although this technique allows carefully controlled testing, the sample preparation and operation of the device is challenging, lowering the overall throughput of testing. Advances in in-situ growth of nanostructures and directed growth of nanostructures should contribute to increase the number of tests that can be performed. This becomes relevant when strength and failure of nanostructures are studied as these phenomena are inherently stochastic, requiring performing several test to achieve reliable statistics.[82]

It should be noted that recently, many other groups have developed MEMS for similar applications, although in-situ TEM operation has not been demonstrated.[93–96] Nanofibers[97] and biological specimens such as collagen fibrils[98] have been tested either in SEM or optical microscopes.

New developments in this type of in situ testing are now being directed to the merging of several physical domains in the same experiment, for example, mechanical, thermal and electrical. For thermal experiments, MEMS have the advantage of achieving higher heating rates and lower thermal drift, due to the low thermal mass of the system. A pioneering example of the use of MEMS for in-situ TEM, temperature-driven experiments, was reported by Zhang et al.[92] where

a microcalorimeter and heater were incorporated into a MEMS in order to measure the size-dependent melting of Bi nanoparticles. Allard et al. also demonstrated an in-situ TEM MEMS heater able to achieve a temperature of 1000°C in 1 ms.[99] More recently, Kang and Saif developed a MEMS device with resistive heating and a bi-metal temperature sensor capable of measuring, during a uniaxial tensile test, the mechanical properties of silicon microbeams from room temperature to 400 °C. They reported a slight decrease of the modulus with increasing temperature, in agreement with previous results.[100]

On the other hand, MEMS with the capability to perform mechanical and electrical measurements either separately[101] or simultaneously[88,95,96] have been recently reported. This should allow probing properties such as piezoelectricity and piezoresistance[96] in the near future. In particular, Espinosa and coworkers have recently developed a four-point microelectromechanical testing system, which combines the aforementioned advantages in mechanical testing with true resistance measurements.[102] In this device, the platform for mechanical testing was extended to accommodate four independent electrical connections to the nanostructure. As shown in **Figure 6**a-b, four traces from the outside electronics are connected to the specimen (Figure 6b). These connections are fabricated on top of insulating freestanding silicon nitride layers[88] to ensure that all electrical signals are independent from each other. The specimen is contacted to by Ion or Electron-Beam-Induced platinum deposition (IBID or EBID) (Figure 6b).

3.2.4. Other Techniques

Other less reported techniques exist for mechanical and electrical testing in situ TEM. They incorporate functionality in a standard TEM grid which simplifies the implementation of the TEM holder and the sample preparation required.

Han et al.[45,103] have used TEM copper grids covered with a collodion thin film (Figure 4e) that bends under electron-beam irradiation as it undergoes polymerization, presumably induced by electron-beam-induced heating. Silicon or silicon carbide (SiC) nanowires are deposited randomly on the grids and get deformed either in tension or bending as the supporting film is deformed under the electron-beam. One important aspect is that the collodion film is able to shrink up to 4–5% which induces large strains in the nanowires, up to 125%.[103] One disadvantage of the method is the lack of measurement of force.

On the other hand, Xu et al.[104] have developed a microfabricated platform for four-point electrical measurements of nanowires (Figure 4f) that can be bonded in a standard TEM single-hole aperture grid. The four probes have a separation of 1 to 2 µm which allows testing the electrical properties of nanowires. With this setup, post-mortem inspection of pretested nanowires can be carried out in TEM. Even when this is not an in situ technique, it could be possible to implement it in situ if the four contacts are addressed with a custom TEM holder.

As a conclusion to this section, we summarize the loading modes, capabilities, resolution and throughput of the techniques that were discussed, in **Table 1**.

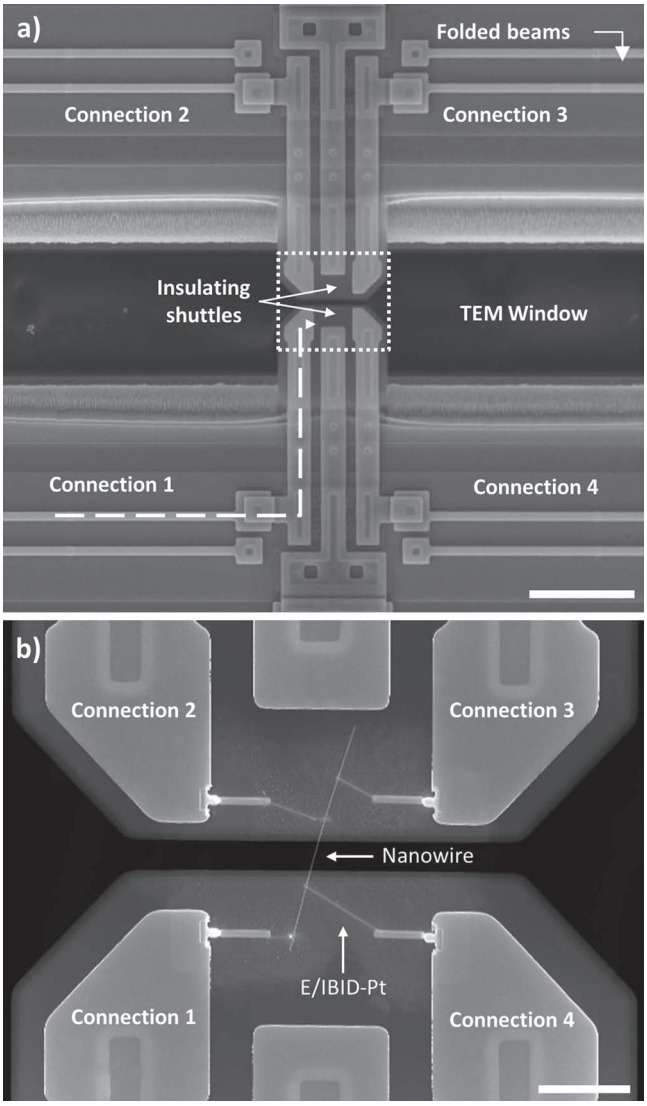

Figure 6. MEMS device for four-point electromechanical measurements. a) Using the same platform shown in Figure 5d, the shuttles of the MEMS device have been modified to perform four-point measurements. Four electrical connections extend on top of insulating silicon nitride shuttles and come close to the specimen. The path of one of the connections is indicated by a dashed line. Scale bar: 40 µm. A detail of the dashed square is provided in b) where a nanowire is connected for four-point measurements using electron and ion beam deposition of platinum. Scale bar 5 µm.[102]

3.3. Sample Preparation for TEM of One-Dimensional Nanostructures

As the reader may appreciate, all of the aforementioned techniques for nanomechanical testing require isolating an individual nanostructure in order to carry out the experiment. Depending on the technique, the sample preparation varies in method and level of difficulty. Here we survey the different methods of sample preparation. Nafari et al.[34] and Costa et al.[68] have also recently reviewed some of the methods described herein. Note also that we review here some techniques that have been applied in other contexts aside from in situ techniques but that are suitable for TEM

small

Table 1. Comparative summary of the loading mode, capabilities, resolution and throughput of several techniques for in-situ TEM mechanical and electromechanical testing of 1D nanostructures. Mechanical Properties are E: Elastic Modulus, σ: Stress, ε: Strain, σ_f: Failure strength, ε_f: Failure strain. Electrical properties are: R: Resistance of specimen and contacts, ρ: Resistivity of specimen.

Method	Loading mode	Measurement Capabilities		Electronic readout in-situ TEM	Force resolution	Testing throughput
		Mechanical	Electrical			
Resonance	Bending	E	N/A	No	N/A	High
TEM/SPM						
Nanoindenter based	Compression/Tension	E, σ, ε, σ_f, ε_f	N/A	Yes	Sub µN	Low
TEM/STM	Bending/Tension	E, ε, ε_f	R	Yes	N/A	High
TEM/AFM	Bending/Tension	E, σ, ε, σ_f, ε_f	R	In some setups	15 nN [80]	Medium
MEMS	Compression/Tension	E, σ, ε, σ_f, ε_f	R, ρ	Yes	12 nN [81]	Low
Straining grid	Tension (not well controlled)	ε, ε_f	N/A	No	N/A	High
Four-point grid	N/A	N/A	R, ρ	No	N/A	Low

sample preparation for mechanical and electromechanical testing.

3.3.1. Random Sample Preparation

For techniques that use a nanomanipulator, tip or electrode to compress, stretch or resonate nanostructures, sample preparation relies on sheer statistics. A large number of specimens are prepared at the same time and a suitable sample is located in situ for the experiment. For carbon nanotubes, a carbon-nanotube-rich fiber, bundle or buckypaper is directly attached to a metallic wire[46,47] or using silver paint to ensure electrical contact.[105–107] A similar method consists of lightly rubbing a wire, previously dipped in silver paste, against carbon-nanotube powder.[108–110] This last method has also been used for boron nitride nanotubes,[67,111] tungsten[112] and zinc oxide nanowires.[78] Alternatively, for the testing of GaN nanowires and InAs nanowhiskers a piece of the growth-substrate was attached directly to one of the electrodes using silver paste.[49,113] A caveat of this technique is that only nanostructures on the edges of the substrate are accessible because of unavoidable small misalignments in the mounting. This means that in order to preserve the nanostructures, proper care needs to be taken in the cutting of the substrate (cleaving is preferred).[34]

Dielectrophoresis has also been used in order to obtain many specimens in a tip that is later attached to the sample holder. Here, an AC voltage is applied between two electrodes while they are immersed in a solution containing the nanostructures, resulting in many of them sticking out of an electrode once the solution dries. This method has been used to prepare CNTs[108] and ZnO nanowires.[114]

3.3.2. Nanomanipulation

We refer to nanomanipulation as the method where an individual nanowire or nanotube is inspected and selected for testing, and later positioned on the testing stage. This technique was originally reported for positioning of nanowires in a MEMS stage for mechanical testing.[81] Here, we review the methods used to position individual nanostructures in the test stages using nanomanipulators either in situ or ex-situ the TEM. We will digress into sample preparation methods that not necessarily target the TEM as a testing instrument because the techniques used to mount nanostructures on stages (even if they are not intended for TEM) can be applicable to TEM if the stage itself can be incorporated in the TEM holder.

Two main manipulation targets — meaning the final destination of the nanostructure — can be identified in the literature: Microfabricated stages or MEMS devices (which may or may not be used in situ the TEM)[3,29,79,82,83,94,96] or in situ TEM holders which have a tip holder.[115]

Manipulation with a testing stage as target proves to be difficult, since the nanostructure has to be attached to two surfaces. Three stages are necessary: first, a suitable nanostructure source is prepared, second a nanostructure is selected and detached from the source with a nanomanipulator and third, the manipulator is used to place the nanostructure on the target set-up (See **Figure 7**a).

For the first stage, most successful results are obtained when the nanostructures are deposited on TEM grids.[3,8,29,79,82,83] They provide a suitable support structure while some portion of the nanostructure sticks out, allowing for manipulation. Nanostructures can be mass-placed in the TEM grid either by sonication followed by drop-casting,[79] or by mechanical exfoliation, achieved by sliding half-cut TEM grids over the substrate or growth source.[2,8,116]

After the nanostructures are in the grid, detachment of the selected specimen is performed. Typically, a very sharp tungsten tip is attached to a manipulator and then is approached to the nanostructure. Once contact is established, some form of attachment needs to be enforced in order to detach or break-off the nanostructure from the grid. It is desirable that the adhesion of the specimen to the tip is greater than what is to the grid.[81,94] This may happen spontaneously depending on the materials and conditions of the sample and manipulator tip but more often Electron Beam Induced deposition (EBID) of an additional material is required.[81] This deposition can be either of residual hydrocarbons in the SEM chamber, resulting in an amorphous carbon deposit,[83] or of other materials such as platinum,[81] copper or tungsten.[117] After attachment of the specimen to

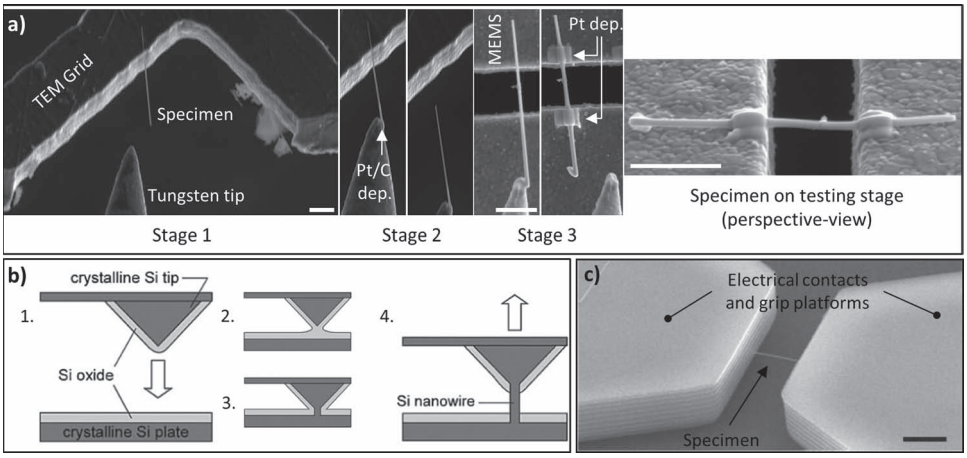

Figure 7. Examples of current and potential sample preparation methods for in situ TEM testing. Figure a) illustrates the sequence of nanomanipulation, where a specimen is transported from a TEM grid to a testing stage with the aid of a nanomanipulator and metal deposition in situ SEM. See text for further details. All scale bars: 2 µm. b) Illustrates in situ TEM specimen preparation, in this case of silicon nanowires. A tip and surface of the same material are brought together and then separated, forming a nanoscale specimen. Reprinted with permission.[73] Copyright 2007, The Japan Society of Applied Physics. c) Illustrates a promising approach for improving testing throughput as yet not implemented for in situ TEM studies. The specimen is grown directly in the testing platforms which ensure good electrical contact and well-defined boundary conditions. Scale bar is 2 µm. Reprinted by permission.[22] Copyright 2006, from Macmillan Publishers Ltd.

the tip is achieved, detachment from the grid is attempted. This requires a careful retraction, or a controlled way of cutting the specimen, for example by electron beam etching.[2] Although focused ion beam (FIB) may be used to perform controlled cutting, its effect on the specimen may be detrimental and should be avoided.

Once the nanostructure is attached to the tip, the manipulator is used to move the tip close to the testing set-up. Careful approach to the target is required, typically using the focus of the SEM to judge depth. By careful approach, one can assess contact when electrostatic attraction of the sample to the surface of the testing set-up occurs. Once contact is established, the nanostructure may be detached from the nanomanipulator if the adhesion to the surface is greater than the adhesion to the tip-nanostructure weld.[81,94] If this is not possible, EBID is used again followed by detachment of the tip. One of the most challenging aspects of this stage of nanomanipulation is judging depth and perspective based on the two-dimensional image of the SEM. A strategy to overcome this difficulty is the patterning of guiding structures in the target.[94]

The nanomanipulation technique may also be applied to mechanical testing of nanostructures in the SPM/TEM Setups. Most of these TEM holders that integrate a nanomanipulator, have the advantage of possessing a detachable tip that can be used for sample preparation ex-situ. Indeed, Asthana et al.[115,118] used a nanomanipulator inside a FIB system to pick a nanowire from the growth substrate and attach it to a tungsten probe, using Ion Beam Induced Deposition (IBID) of tungsten. After this, the tip is mounted on a STM/TEM-type in situ TEM holder. Under this methodology of preparation, ZnO nanobelts and titanium dioxide nanotubes[118] were tested.

3.3.3. Other Techniques

Other techniques have been used for TEM sample preparation. They include in situ sample preparation, and directed growth or cofabrication of the nanostructure in the testing set-up.

For the first method, samples are in situ prepared for testing using a combination of mechanical forces and adhesion. Kizuka et al.,[74] Luo et al.,[119] and Moore et al.[120] used a nanomanipulator tip in situ TEM in order to press a surface of the material of interest. Retraction of the tip causes pulling of the material in a nanowire shape that although not very well defined, is narrow, long and with very small dimensions (See Figure 7a). Silicon nanowires with extremely high fracture strains (30%),[74] superelongation (200%) of metallic glasses at room temperature[119] and superplastic (elongation 280%) salt nanowires[120] were demonstrated using this approach. The point contacts mentioned in section 2.2.2.3 are fabricated using this method.

Using a combination of the random dispersion method and in situ sample preparation, Lu et al. demonstrated cold-welding of gold nanowires.[121] They started with ultrathin nanowires prepared by a chemical method, attached them to a nanomanipulator tip and to an opposing wire using methods similar to those outlined in section 2.3.1. When two of these ultrathin nanowires are brought into contact they cold-weld together by applying pressures of less than 4.7 MPa, much lower than typical cold-welding of bulk metals. The welded nanowire does not have grain boundaries or additional defects and this was demonstrated by electrical and mechanical measurements where the current conduction was not affected by the welding, and the nanowires fractured in a different location far from the weld. Another type of attachment mechanism is the amorphous carbon produced by concentrating the TEM beam in a very small area.[122,123]

In general, in-situ specimen preparation has demonstrated to be useful in order to test small sized samples (<10 nm) which are typically employed in testing fundamental phenomena, such as quantized conduction.[52] However, the

technique is not amenable for testing batch-produced nanotubes or nanowires — used in the majority of demonstrations of new electronic devices — and therefore its applicability is limited.

Directed growth is an alternative for sample preparation where the nanostructure is cofabricated with the specimen or grown directly in the testing setup. It has advantages because it may lead to more robust boundary conditions of the specimen. Moreover, electron-beam-deposition processing steps are avoided, lessening the potential for sample contamination.[48] In addition, there is the potential to improve throughput. Liu et al.[48] were able to growth tungsten oxide nanowires in tungsten tips. These tips were later used inside the TEM as one of the electrodes in the resonance technique. This technique was remarkable as they were able to test nanowires as small as 16 nm obtaining atomic resolution and characterization of the specimens under investigation. They discovered that the modulus of tungsten oxide nanowires increases as much as 300% for small samples. In a similar approach, but not in situ TEM, He and P. Yang[22] (see Figure 7c) grew sub-100 nm silicon nanowires between two separate platforms that were used to later uniaxially stretch the nanowires while measuring their current-voltage response, providing the first evidence of size-dependent piezoresistance of silicon nanowires. In both cases, TEM inspection of the samples was performed confirming the suitability of the electrical (ohmic) and mechanical boundary conditions (clamped). This setup was later used to carry out mechanical bending experiments using AFM.[124] Overall, although directed growth is an attractive approach, many challenges remain in order to be able to grow and test the full spectrum of materials (metallic, semiconducting, CNTs) in this fashion. The particular synthesis and processing conditions will need to be investigated for each material and may conflict with other parts of the microfabrication of the testing setup.

In terms of cofabricated samples, strictly speaking, one-dimensional nanostructures have not been tested in situ TEM. Instead, only very thin films of aluminum[85,87] and silicon[125] have been studied. However, advancements in the minimal sample dimension that is obtainable in this microfabrication top-down approach[126] may allow the testing of true one-dimensional nanostructures in the near future.

4. Capabilities of In-Situ TEM Applied to One-Dimensional Nanostructures

It was mentioned in the introduction that TEM is the technique-of-choice in order to perform appropriate measurements of the mechanical properties of nanowires and nanotubes. Up to this point we have given an overview of the experimental techniques and sample preparation methods that allow the testing of nanostructures in situ the TEM. In this section, we aim to illustrate with specific examples why TEM gives superior measurements of mechanical and electromechanical properties.

As mentioned before, high spatial resolution is the most obvious advantage of TEM since defects and atomic structure can be identified and correlated to the mechanical properties. Even at low magnification, TEM can provide unique information about the collective motion of defects, for example, the nucleation of multiple zones of dislocation activity in penta-twinned silver nanowires.[84] At high magnification, individual defects (point and extended), fracture surfaces and planes, among others, can be identified.

However, TEM allows for a number of other analytical techniques, which coupled to its resolution allow the thorough characterization of one-dimensional nanostructures. In this section, we aim to illustrate examples where these extra capabilities have played a role in determining the mechanical and electromechanical properties of 1D nanostructures. Clearly, nanostructure characterization in TEM has been carried out in several other cases, but we limit ourselves here to examples where it has been used in conjunction with mechanical or electromechanical testing.

4.1. High-Resolution TEM

High-resolution is, perhaps, the most clear advantage of TEM. As such, we aim in this section to provide a few case studies where the use of HRTEM was critical to obtain conclusions related to mechanical or electromechanical behavior. In particular, we highlight a few examples where the high resolution of TEM was directly linked to measurements leading to a structure-properties correlation. We first present examples on mechanical and electromechanical characterization of nanotubes followed by studies on nanowires. The most prominent advantages of HRTEM in mechanical and electromechanical testing are the identification of preexisting defects, the precise quantification of load and the current or load-bearing area, and the imaging of the failure mechanisms with atomic resolution.

4.1.1. In situ HRTEM Testing of Nanotubes

The majority of in situ electromechanical TEM studies at high resolution have focused on carbon nanotubes. Fracture surfaces, kinks and their atomic structure under deformation have been reported. Here, we highlight studies in which a direct correlation was demonstrated between measured properties and high-resolution imaging.

In terms of mechanical properties, measurements of modulus, fracture strength, and elucidation of the fracture mechanisms were achieved. One of the earliest examples was given by Poncharal et al.[47] They measured the elastic modulus of CNTs for several diameters using the electromechanical resonance method. It was reported that the elastic modulus for very thin CNTs agreed with theoretical estimates of 1 TPa while for diameters greater than 12 nm there was a sharp transition and the measured modulus dramatically decreased to around 100 GPa for larger diameters. However, HRTEM revealed that CNTs of larger diameter developed a waving/rippling of the shells when they undergo large bending deformation (see **Figure 8**a). This provided an explanation for the decrease in modulus for large diameters, as a result not of material-property degradation with size, but of a change in the deformation mode.

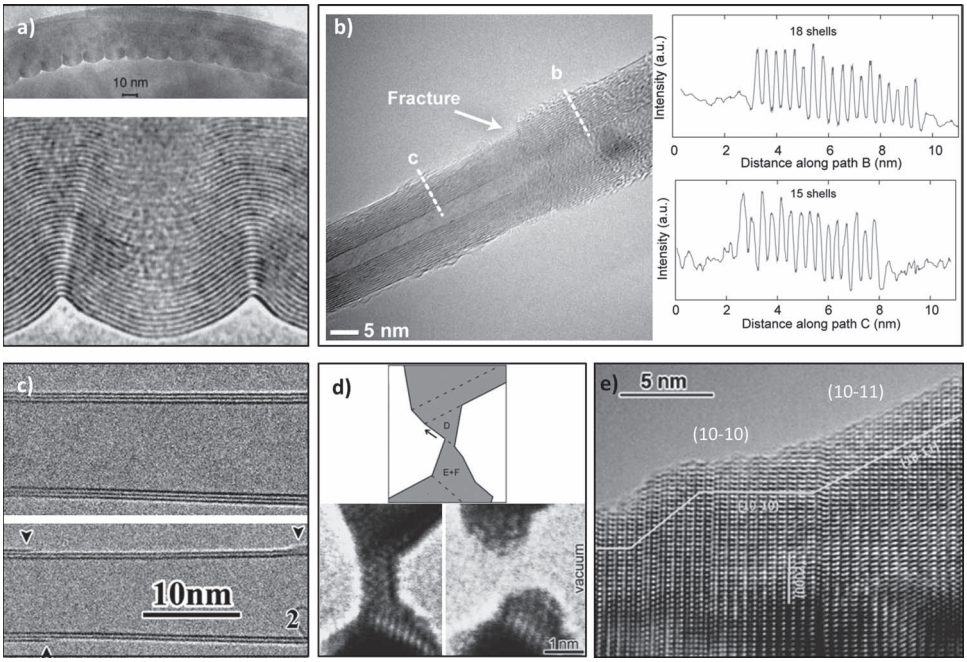

Figure 8. HRTEM capabilities applied to several electromechanical characterizations of nanostructures. a) Observation of bending-induced kinking in multi-walled CNTs (MWCNT). Reprinted with permission.[47] Copyright 1999, AAAS. b) Identification of number of shells fractured in a tensile test of a MWCNT. Reprinted with permission.[3] Copyright 2008, Nature Publishing Group. c) Shell-by-shell current-induced failure of MWCNTs. Reprinted with permission.[63] Copyright 2005, the American Physical Society. d) Observation of slip (indicated by an arrow) occurring as a precursor to failure in palladium nanocontacts. Reprinted with permission.[72] Copyright 2009, The Japan Society of Applied Physics. e) Identification of fracture planes in GaN nanowires subjected to uniaxial compression. Reprinted with permission.[59] Copyright 2011, American Chemical Society.

More recently, Peng et al.[3] measured the fracture strength of multi-walled CNTs (MWCNTs) in situ TEM using a MEMS-based tensile testing device. Here, observation of the number of fractured shells in the nanotube was possible, providing an unambiguous and precise measurement of the load-bearing cross-sectional area (see Figure 8b). Sword-in-sheath failure was observed, in which fracture of only one (or in some cases a few) of the load-bearing shells of the MWCNT occurred. The number of fractured shells was found to increase when the MWCNTs were subjected to increasing doses of electron irradiation which introduced covalent crosslinking defects between shells. These findings proved the benefits of irradiation-induced cross-linking on the load-bearing capabilities of MWCNTs. In this case HRTEM observation of the number of fractured shells was a critical requirement for the accurate interpretation of the experimental data.

A similar study, this time carried out with a STM/TEM setup, demonstrated a sword-in-sheath fracture mechanisms for tungsten-disulfide (WS_2) nanotubes.[127] In this work, the authors performed some of the testing in situ SEM which does not allow for the direct and unambiguous identification of the failure mechanisms, thus exemplifying the contrast between TEM and SEM in terms of resolution and suitability of the techniques for mechanical testing of nanostructures.

Recently, Filleter et al.[83] carried out an in-situ TEM study on double-walled CNT (DWCNT) bundles. Again the direct observation of failure mechanisms of the bundles was critical in understanding the effect of electron irradiation dose. Here, by directly measuring the number of CNTs across the diameter of the bundles, the effective modulus was accurately determined and was found to increase by up to one order of magnitude (30–60 GPa to 693 GPa) at an optimal dose of $8.9 \pm 0.3 \times 10^{20}$ e/cm^2. Moreover, a transition between sword-in-sheath and full cross-section failure was observed, demonstrating the benefits of crosslinking in promoting the full utilization of the CNTs at the bundle level. Likewise, the effective strength increased from 2–3 GPa to 17.1 GPa at a dose of $11.3 \pm 0.3 \times 10^{20}$ e/cm^2. Such significant improvement in mechanical performance at higher levels of hierarchy in CNT based materials, suggests promise in developing macroscopic materials that approach the exceptional properties of individual nanostructures.

In the context of electrical properties, a very compelling example of the power of HRTEM was provided by Huang et al.[63] They imaged the wall-by-wall breakdown of a MWCNT when a critical current density was applied to it (see Figure 8c). Discrete jumps in the current through the MWCNT were directly correlated with one-by-one shell failure. Interestingly, they were able to establish that failure does not necessarily progresses from the outer to the inner shells but rather in an alternate way in which outer-to-inner and inner-to-outer breakdown sequences are possible. These findings, which have only become possible by the direct visualization, provided by in-situ TEM, may have significant implications on the use of CNTs in electronic devices.

4.1.2. In situ HRTEM of Crystalline Nanospecimens

Several electromechanical studies of crystalline nanospecimens have been carried out in situ TEM, including nanowires

small

of metallic and semiconducting materials and point junctions in metallic specimens. Perhaps the most striking example of the use of HRTEM in electromechanical experiments is given by experiments using break junctions were specimens of atomic width have been tested. These types of specimens are fabricated by putting a tip in contact to an opposing surface of the same material and carefully retracting the tip. A review of this work is given in,[128] here we present some relevant examples.

In a classic paper, Ohnishi et al.[52] fabricated break junctions of gold, and stretched the junctions so that the cross–section was reduced by one row of atoms at a time. They simultaneously measured the conductance of the junction demonstrating that it is quantized by the unit conductance $G_0 = 2e^2/h$ where e is the electron charge and h is the Planck's constant. As the cross-section reduced by one row of atoms, the conductance reduced by one unit of G_0. Here, HRTEM was critical to establish the number of atomic rows present in the specimen. The width of the specimen was established by direct imaging because the crystalline structure allowed counting atomic rows. The depth of the specimen was estimated from the gray intensity present in the images.

The majority of these experiments were carried out in a STM/TEM configuration (see section 2.2.2) meaning that force was not measured; however, recently T. Kizuka and coworkers developed a TEM/AFM with real time measurement capabilities,[70] which allows force measurements. With this setup they were able to test metallic and semiconducting specimens, specifically silicon wires of nanometer width,[73,74] and copper and palladium nanocontacts.[71,72] In terms of HRTEM, their last work is very insightful in the sense that several domains (grains), few atoms wide, were directly imaged and their evolution, as a function of strain, was imaged. In particular, it was established that grain evolution was dominated by slip events (see Figure 8d). The discrete nature of the events, where the slip distance is a multiple of the lattice constant, was captured. The final stage consisted of a single crystal pillar, which failed in shear. This allowed the accurate measurement of the critically-resolved shear stress for palladium (0.3–0.4 GPa).

On the other hand, for nanospecimens synthesized by chemical methods such as nanowires, HRTEM has been used for establishing the cross-section of the specimens and for imaging the lattice distortions caused by mechanical deformation.[79] TEM also enables accurate determination of the cross-section of the specimen[49] because it allows the differentiation of the specimen's atomic structure from surface contaminants, which in other imaging techniques may appear to be part of the specimen. Additionally, combined with diffraction and a knowledge of the crystalline structure of the specimen material, the exact orientation of the specimen can be established.[29]

In terms of the lattice distortion caused by applied strain, examples have been reported for SiC,[45] Si,[103] and GaN nanowires.[59] In all of these cases, imaging of individual dislocations and measurement of the Burgers vector and circuit was possible. Furthermore, the evolution from pristine structure, to nanowires containing dislocations and leading to amorphization or fracture (see Figure 8e), was clearly observed.

4.2. Diffraction

The different modes of diffraction in TEM give useful information about crystal structure, lattice spacing and strain, and presence or nucleation of defects in the sample. In addition, TEM allows probing very small volumes enabling local measurements within a nanostructure. In particular, selected-area electron diffraction (SAED) has a strain resolution of up to 0.1%,[129] nano-beam electron diffraction (NBED) can probe an even smaller (few nanometers) region with 0.06% strain resolution[129] and convergent beam electron diffraction (CBED) provides 0.02% strain resolution. Diffraction also has advantages in terms of structural characterization and defect identification. A diffraction pattern can reveal twining, phase changes and amorphization. Subtle defects that are difficult to locate in bright-field imaging (even at high resolution) like inversion domain boundaries (IBD) — important for correlation to piezoelectric response[40] — can be identified by comparing simulated and experimental results from CBED patterns.[130]

Despite the various capabilities of diffraction in TEM, it has to date been used mostly for strain measurements and crystalline characterization in the mechanical testing of nanowires. However, it is a very promising in-situ approach to reveal novel electromechanical phenomena in future studies.

For the determination of strain, SAED has been used in the mechanical testing of nanowires and nanobelts. Agrawal et al.[79] acquired diffraction patterns of ZnO nanowires while they were uniaxially tensioned. The local strain obtained from diffraction was compared to the overall strain obtained from bright-field measurements of the change in length of the gage region. The difference between the two strains was comparable to the experimental error, proving that the experimental setup imposed uniaxial-tensile boundary conditions and that there was no slippage between the nanowire and the shuttles in the microsystem (see **Figure 9**a-c). Similarly, Vaughn and Kordesch[131] used a TEM holder with an embedded manipulator to deform gallium oxide nanobelts and observed diffraction patterns as a function of deformation. They were able to measure the change in the a and c spacings of the monoclinic lattice with angstrom-scale precision.

On the other hand, Han et al.[45] performed SAED on the highly deformed parts of silicon carbide (SiC) nanowires, proving the amorphization of the nanowires, which took place at large strains. Halo-ring segments on the patterns revealed the development of amorphous regions in the sample and dark-field-imaging allowed their visualization. In a similar fashion, Asthana et al.[78] observed the amorphization of ZnO nanowires under repeated bending loads. High resolution TEM images showed the deformation of the lattice and SAED patterns allowed the confirmation of this amorphization, as well as the nucleation of defects, evidenced by streaks and arc-like diffraction spots.

For CNTs, the chirality of the specimens under test can be determined using SAED[3] (See Figure 9d-f). Intensity profiles of principal layer lines (l_1, l_2, l_2 in Figure 9d-f), common in diffraction patterns of CNTs, are fitted to Bessel functions, which order can then be related to the chiral index.[132]

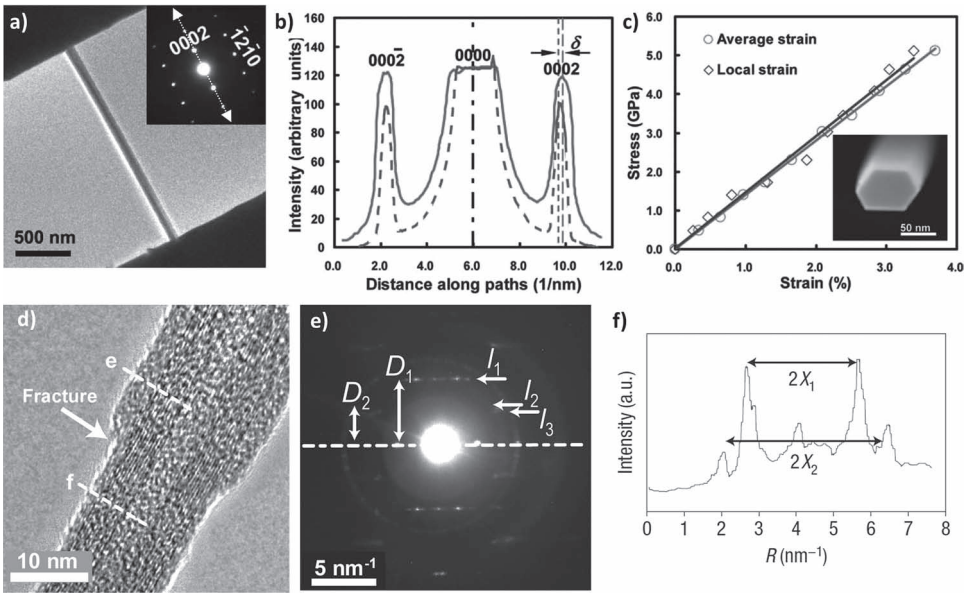

Figure 9. Use of diffraction capabilities in the TEM to perform mechanical characterization. Figures a-c) correspond to uniaxial testing of ZnO nanowires. Figure a) shows the TEM image of the nanowire being pulled at two ends and its diffraction pattern. An intensity profile along the indicated path is shown in b). The peaks indicate the position of the diffraction spot, which shifts by a reciprocal distance δ as a result of strain. Local strain can be computed from measurement of δ. Comparison of this local strain with the average strain (c) allows discarding slippage effects in the grips of the tensile-testing device. Reprinted with permission.[79] Copyright 2008, American Chemical Society. Figures d-f) correspond to uniaxial testing of MWCNTs. Figure d) shows the HRTEM image of the fractured nanotube, while e) shows the corresponding diffraction pattern. The intensity profile along I_1 (f) can be fitted to Bessel functions and the chirality of the nanotube can be determined. Reprinted with permission.[3] Copyright 2008, Nature Publishing Group.

Although not currently employed for in-situ electromechanical characterization, emerging TEM diffraction techniques are noteworthy because of their capability of localized probing. In particular, Diffraction Scanning Transmission Electron Microscopy (D-STEM), combined with precession electron microscopy,[133,134] is capable of obtaining a diffraction pattern from an area as small as 3 nm in characteristic dimension. More interestingly, it has been automated so that many individual diffraction patterns can be obtained throughout the sample, in a pixel-by-pixel fashion.[133] Such high-resolution, automated mapping of crystalline structure has been used to characterize grain boundaries in copper interconnects as small as 70 nm, revealing the change in crystalline texture as interconnects are downscaled.[134] One can envision this technique employed for in-situ mechanical experiments both previous to the experiment, e.g. in order to fully characterize atomic structure before deformation, and during the test, in order to elucidate strain distributions and their effect on preexisting or engineered defects, e.g., coherent twin boundaries.

4.3. Analytical Techniques

The interaction of impinging electrons with atomic structures produces several sub-products and physical phenomena that are used for analytical purposes. Taking advantage of this, the TEM can be used to carry out spectroscopy and other types of analytical measurements. Using X-ray electron dispersive spectroscopy (EDS) elemental analysis of the specimen can be carried out with a resolution of a few nanometers depending on the thickness of the sample.[14] Furthermore, electron energy loss spectroscopy (EELS) gives elemental information, as well as information on the bonding and thickness of the sample.[14] The resolution of these techniques in the TEM is of particular relevance when nanostructures are tested, as local effects can be probed accurately.

In the framework of mechanical characterization, analytical TEM has been used to characterize the change in chemical bonding as a function of deformation, the diffusion of material within the specimen as it is strained, and to characterize the shape and cross-sectional areas used to calculate stresses from measured forces.

In the context of chemical bonding studies, Aslam et al.[109] analyzed the EELS spectra of single-walled carbon nanotube bundles as they were bent and buckled under compressive load. In particular, they investigated the dependence of the ratios of π and σ covalent bonding (represented by the peaks π^* and σ^* in the EELS spectra) as reversible and irreversible deformation was imposed on the bundles. The ratio $\pi^*/(\pi^* + \sigma^*)$ increased in reversible deformation showing that the overlap of the σ bonds decreased, created by the nonplanarity induced by the applied strain. When irreversible deformation was imposed and permanent defects were introduced in the bundle, the ratio $\pi^*/(\pi^* + \sigma^*)$ decreased, revealing a decrease of the π bonding, resulting from non-hexagonal defects being introduced in the structure of the CNT.

In the same vein, Han et al.[45] analyzed EELS spectra of silicon carbide (SiC) nanowires in order to establish the appearance of an amorphous phase under large strain

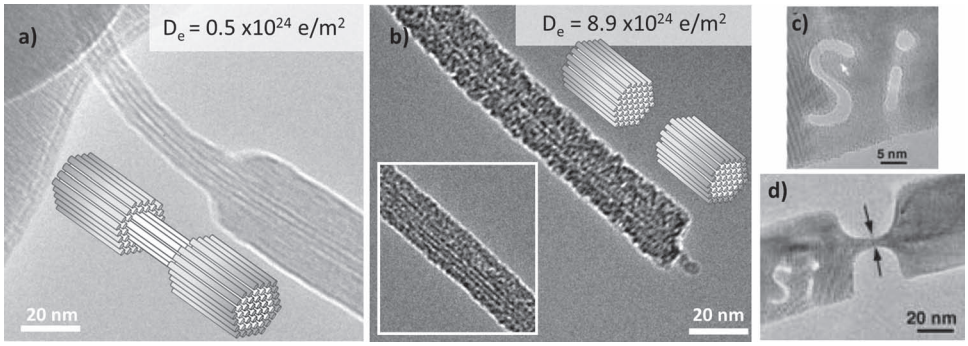

Figure 10. Examples of in situ TEM specimen modification of samples and its potential application in mechanical problems. Figures a,b) illustrate the in situ irradiation of carbon-nanotube bundles. With a low irradiation dose (a) the fracture occurs at low effective-stress levels and in a sword-in-sheath mode. By increasing the electron irradiation (b) the load-carrying capacity of all the shells in the nanotubes is utilized, resulting in higher effective fracture strengths and a brittle-like failure. Adapted with permission.[83] Electron irradiation may also be used to selectively remove material in the specimen. Figures c) and d) show a silicon nanowire where letters and a dog bone shape have been patterned with the high-intensity electron beam in the TEM. These modifications could potentially be used in tensile testing and determination of stress-intensity factors at the nanoscale. Adapted with permission.[122]

plasticity. Comparing to EELS spectra of crystalline SiC, they demonstrated that the broadening of some peaks corresponds to the manifestation of an amorphous phase in the highly strained region of the nanowire. Further demonstration of this amorphous phase was established by diffraction studies.

The same group also applied the EELS and EDS techniques to analyze the large-strain plasticity of silicon nanowires and demonstrated that oxygen diffusion did not drive this process. While straining the nanowire, several EELS spectra were taken across the diameter of the specimen. The results show that a silicon oxide layer (which natively covers the silicon nanowires) does not migrate to the center of the wire while it is strained. Complementary elemental EDS spectra showed similar results. This helped establish that large strain plasticity was, in fact, driven by dislocation nucleation, which led to a disordered atomic structure, and not by oxygen diffusion.

Filleter et al.,[83] Bernal et al.,[29] and Richter et al.[135] used EELS thickness maps in order to obtain information about the cross section of the specimens under in-situ testing. Filleter et al.[83] applied this technique in the tensile testing of double-walled carbon nanotube bundles in order to establish their circular cross-section, therefore supporting the model applied for calculating stresses in the specimen. In a similar fashion, Bernal et al.[29] confirmed the geometry used for calculating stresses in GaN nanowires by comparing an EELS thickness map of the specimen to the expected thickness resulting from a polygonal-cross-section specimen. Richter et al.[135] used the same technique to establish the octagonal cross-section of copper nanowhiskers, although the tensile tests were not carried out in situ TEM.

4.4. In situ Specimen Modification

Another advantage of in-situ TEM experiments is that in some cases the high-energy electron beam can also be used to advantageously modify the specimen under investigation in-situ the TEM, followed by mechanical characterization. Due to the high resolution of the TEM and the precise control of atomic modifications, new avenues are opened for the testing of mechanical systems based on nanostructures.

One of the most relevant examples is the use of electron irradiation to achieve covalent cross-linking of carbon nanotubes and shells inside multiwalled carbon nanotubes[3] and carbon nanotube bundles[83,136] (**Figure 10**a-b). The high-energy electron beam induces knock-off of atoms in the nanotube shells creating structural and interstitial defects that link adjacent shells (in the case of a multiwalled tube) and adjacent nanotubes (in the case of nanotube bundles). As alluded to before, this in situ modification has been shown to significantly increase the effective strength and stiffness of these carbon materials opening an avenue for their most effective use in nanocomposites and macroscopic fibers.[17] Although many reports exist on the modification of carbon based materials using electron irradiation,[137] the modification of crystalline materials and the mechanical effects or irradiation on nanowires remains relatively unexplored.

Although mechanical tests were not carried out, an interesting example of nanowire modification is given by Xu et al.[122] By focusing a 200 keV TEM beam in a few-nanometers spot they achieved current densities ranging from 10^3 to 10^6 A/cm^2 passing across the specimen. This was used to create a variety of very controlled shapes such as holes, letters, dogbone specimens and to generate welds between nanowires of several materials, namely, silicon, gold, copper, silver and tin (Figure 10c-d). This type of technique may be useful to expand the possibilities of testing beyond the usual tension, compression and bending experiments. One can envision, for example, the creation of pre-cracked specimens in order to compute stress intensity factors at the nanoscale or to trigger failure at a certain location in the specimen while simultaneously performing high resolution imaging.

5. Summary and Outlook

In this review, we have illustrated how in situ TEM has played a fundamental role in the characterization of mechanical and

electromechanical properties and associated phenomena in one dimensional nanostructures. The unique atomic-scale resolution, analytical, and spectroscopic capabilities of TEM, combined with a variety of in-situ mechanical and electromechanical experimental setups has allowed the achievement of several milestones in the study of one-dimensional nanostructures. Among the most relevant and impactful are the measurement of the elastic modulus[47] strength[3] and superplasticity of CNTs,[62] the experimental observation of quantized conductance in atom-sized specimens,[52] the identification of size-scale effects in the elastic properties on nanowires[29,79] and the measurements of room-temperature large-strain plasticity in silicon an silicon carbide nanowires.[45,103]

We have shown that the experimental setups have evolved in complexity, starting from relatively simple two-electrode systems to produce resonance in nanostructures, to more sophisticated systems with in situ TEM manipulators to achieve nanostructure deformation, force measurements and electrical addressing, ending in complex lab-on-a-chip MEMS approaches, where nanoscale tensile and compressive devices are used to impose and measure forces acting on the nanostructures. One pattern emerging is the compromise that exists between experimental complexity and testing throughput. Although MEMS-based testing offers the best control of boundary conditions in a mechanical or electromechanical test, sample preparation is more challenging and set-up complexity is greater, leading to a lower overall testing throughput. This explains the greater number of reports on nanostructure testing using the TEM/SPM approaches which, at the expense of sometimes compromising homogeneity of applied deformation (by inducing buckling or bending) allow the realization of more tests in less time. In the medium term, the appearance of more groups working on MEMS-based characterization and the development of new specimen preparation techniques will most likely reverse this trend. Nevertheless, TEM/SPM will continue to be an important technique given the wide availability of commercial implementations, which lowers the entry-barrier for new researchers.

For all implementations, continuous instrumentation improvements are necessary to obtain better results. In the TEM, the CCD capture rate (~ms) is a limiting factor in carrying out experiments that require a higher sampling rate. Approaches such as beam deflection to a segmented CCD[36] have been implemented, but a limitation still exists to capture a large number of images in fast times. For the testing setups, achievement of true-displacement control in tensile testing may allow observing phenomena where sudden drops in the force-displacement behavior of the specimen occurs, such as phase transformations[82] and discrete dislocation yield events.[138] Additionally, electronic bandwidth, and its inverse correlation with drift and noise[80] can hinder the realization of dynamic experiments when nN-scale loads are measured electronically, or when nA currents and μV voltages are passed through the specimen. For instance, assuming motion at 10% the speed of sound, the characteristic time of dislocation motion is of the order of 1–10 ns in a 100 nm nanowire. Although such bandwidth is reachable in conventional electronic devices, high-speed measurements of the smaller signals involved in the measurements of nN loads, would require specialized, on-chip, electronics.

A common challenge in all methods will continue to be the reduction of constraints, geometrical or of other kinds, so that the full capabilities of TEM can be employed in the testing of nanostructures. Double-tilting remains to be widely utilized which is illustrative of the still-untapped potential of TEM to discover more new phenomena in nanostructures. Incidentally, TEM/SPM double-tilt holders have been very recently made commercially available.[139] Similarly, the development of new MEMS and TEM/SPM approaches which allow coupled mechanical and electrical testing[88,96] will likely shift the focus of this field from purely mechanical tests, to studies which probe electromechanical phenomena such as piezoelectricity and piezoresistivity of nanostructures.

Furthermore, we stress that merging of state-of-the-art TEM techniques with in-situ experiments will likely result in the discovery of previously unobserved phenomena. For example, techniques such as D-STEM with the capability of automated, localized crystalline characterization can prove critical to identify preexisting defects and strain distributions. Dynamic and ultrafast TEM[35,36] (DTEM and UEM) could potentially be used to observe dislocation motion as a function of strain rate. High-strain-rate experiments in nanostructures remain an unexplored area of research, even when presumably it is of high relevance given its influence on the deformation of some metallic systems[56] and the fact that mechanical and electromechanical applications for nanostructures will likely impose MHz or GHz cycling.[1] In this regard it should be noted that the current MEMS-based methods discussed herein, can in principle approach testing rates at least in the kHz regime. Furthermore, although bridging of spatial scales between nanostructure computational simulations and experiments has been achieved to some extent,[79,84] the bridging of strain-rate will likely provide many insights into the suitability of the currently-used atomistic approaches for nanomaterial modeling, such as molecular dynamics.

Acknowledgements

HDE acknowledges the support of the NSF through award No. DMR-0907196, ONR through award No. N00014-08-1-0108, and ARO through MURI award No. W911NF-09-1-0541. We thank Dr. Allison Beese for critical review of the manuscript and helpful discussions. We thank the anonymous reviewers for insightful suggestions and comments that have improved the article.

[1] C. Rutherglen, D. Jain, P. Burke, *Nat. Nano* **2009**, *4*, 811–819.
[2] M. Naraghi, T. Filleter, A. Moravsky, M. Locascio, R. O. Loutfy, H. D. Espinosa, *ACS Nano* **2010**, *4*, 6463–6476.
[3] B. Peng, M. Locascio, P. Zapol, S. Li, S. L. Mielke, G. C. Schatz, H. D. Espinosa, *Nat. Nanotechnology* **2008**, *3*, 626–631.
[4] J.-C. Charlier, X. Blase, S. Roche, *Rev. Modern Phys.* **2007**, *79*, 677.
[5] Y. Sun, B. B. Gates Mayers, Y. Xia, *Nano Lett.* **2002**, *2*, 165–168.
[6] P. Yang, R. Yan, M. Fardy, *Nano Lett.* **2010**, *10*, 1529–1536.

[7] S. Xu, Y. Qin, C. Xu, Y. Wei, R. Yang, Z. L. Wang, *Nat. Nano* **2010**, *5*, 366–373.
[8] O. Loh, X. Wei, C. Ke, J. Sullivan, H. D. Espinosa, *Small* **2010**, *7*, 79–86.
[9] M. S. Arnold, A. A. Green, J. F. Hulvat, S. I. Stupp, M. C. Hersam, *Nat. Nano* **2006**, *1*, 60–65.
[10] L. Wei, M. L. Charles, *J. Phys. D* **2006**, *39*, R387.
[11] E. Koren, J. K. Hyun, U. Givan, E. R. Hemesath, L. J. Lauhon, Y. Rosenwaks, *Nano Lett.* **2011**, *11*, 183–187.
[12] D. Tham, C. Y. Nam, J. E. Fischer, *Adv. Funct. Mater.* **2006**, *16*, 1197–1202.
[13] J. E. Allen, E. R. Hemesath, D. E. Perea, J. L. Lensch-Falk, Z. Y. Li, F. Yin, M. H. Gass, P. Wang, A. L. Bleloch, R. E. Palmer, L. J. Lauhon, *Nat. Nano* **2008**, *3*, 168–173.
[14] D. B. Williams, C. B. Carter, *Transmission Electron Microscopy: A Textbook for Materials Science*, 2nd ed., Springer, New York **2009**.
[15] *Electron Microscopy of Nanotubes* (Eds: Z. L. Wang, C. Hui), Kluwer Academic Publishers, Norwell, **2003**.
[16] *Handbook of Microscopy for Nanotechnology* (Eds: N. Yao, Z. L. Wang) Kluwer Academic Publishers, New York **2005**.
[17] H. D. Espinosa, T. Filleter, M. Naraghi, *Adv. Mater.* **2012**, *24*, 2805–2823.
[18] Z. L. Wang J. Song, *Science* **2006**, *312*, 242–246.
[19] Y. Qi, N. T. Jafferis, K. Lyons, C. M. Lee, H. Ahmad, M. C. McAlpine, *Nano Lett.* **2010**, *10*, 524–528.
[20] Y. Gao Z. L. Wang, *Nano Lett.* **2009**, *9*, 1103–1110.
[21] Y. Qi, J. Kim, T. D. Nguyen, B. Lisko, P. K. Purohit, M. C. McAlpine, *Nano Lett.* **2011**, *11*, 1331–1336.
[22] R. R. He, P. Yang, *Nat. Nanotechnol.* **2006**, *1*, 42–46.
[23] Y. Zhu, F. Xu, Q. Qin, W. Y. Fung, W. Lu, *Nano Lett.* **2009**, *9*, 3934–3939.
[24] J.-H. Zhang, Q.-A. Huang, H. Yu, J. Wang, S.-Y. Lei, *J. Appl. Phys.* **2009**, *105*, 086102.
[25] J. S. Milne, A. C. H. Rowe, S. Arscott, C. Renner, *Phys. Rev. Lett.* **2010**, *105*, 226802.
[26] I. Ryu, J. W. Choi, Y. Cui, W. D. Nix, *J. Mech. Phys, Solids* **2011**, *59*, 1717–1730.
[27] C. E. Carlton, P. J. Ferreira, *Micron* **2012**, DOI: 10.1016/j.micron.2012.03.002.
[28] C. E. Carlton, P. J. Ferreira, *Microscopy and Microanalysis* **2009**, *15*, 736–737.
[29] R. A. Bernal, R. Agrawal, B. Peng, K. A. Bertness, N. A. Sanford, A. V. Davydov, H. D. Espinosa, *Nano Lett.* **2010**, *11*, 548–555.
[30] P. J. Ferreira, K. Mitsuishi, E. A. Stach, *MRS Bull.* **2008**, *33*, 83–85.
[31] J. Cummings, E. Olsson, A. K. Petford-Long, Y. Zhu, *MRS Bull.* **2008**, *33*, 101–106.
[32] K. W. Urban, *Science* **2008**, *321*, 506–510.
[33] M. Legros, D. S. gianola, C. Motz, *MRS Bull.* **2010**, *35*, 354–360.
[34] A. Nafari, J. Angenete, K. Svensson, A. Sanz-Velasco, H. Olin, in *Scanning Probe Microscopy in Nanoscience and Nanotechnology* (Ed: B. Bhushan), Springer, New York **2011**.
[35] J. S. Kim, T. LaGrange, B. W. Reed, M. L. Taheri, M. R. Armstrong, W. E. King, N. D. Browning, G. H. Campbell, *Science* **2008**, *321*, 1472–1475.
[36] A. H. Zewail, *Science* **2010**, *328*, 187–193.
[37] M. R. Armstrong, K. Boyden, N. D. Browning, G. H. Campbell, J. D. Colvin, W. J. DeHope, A. M. Frank, D. J. Gibson, F. Hartemann, J. S. Kim, W. E. King, T. B. LaGrange, B. J. Pyke, B. W. Reed, R. M. Shuttlesworth, B. C. Stuart, B. R. Torralva, *Ultramicroscopy* **2007**, *107*, 356–367.
[38] D. S. Yang, C. S. Lao, A. H. Zewail, *Science* **2008**, *321*, 1660–1664.
[39] H. D. Espinosa, R. A. Bernal, M. Minary-Jolandan, *Adv. Mater.* **2012**, DOI: 10.1002/adma.201104810.
[40] H. Morkoç, *Handbook of Nitride Semiconductors and Devices*, Vol. *1*, Wiley-VCH, Weinheim, Germany **2008**.
[41] I. Levin, A. Davydov, B. Nikoobakht, N. Sanford, P. Mogilevsky, *Appl. Phys. Lett.* **2005**, *87*, 103110–3.
[42] Y. Ding, Z. L. Wang, *Micron* **2009**, *40*, 335–342.
[43] K. H. Lee, J. Y. Lee, Y. H. Kwon, T. w. Kang, J. H. You, D. U. Lee, T. Kim, *J. Mater. Res.* **2009**, *24*, 3032–3037.
[44] B. W. Jacobs, M. A. Crimp, K. McElroy, V. M. Ayres, *Nano Lett.* **2008**, *8*, 4353–4358.
[45] X. D. Han, Y. F. Zhang, K. Zheng, X. N. Zhang, Z. Zhang, Y. J. Hao, X. Y. Guo, J. Yuan, Z. L. Wang, *Nano Lett.* **2007**, *7*, 452–457.
[46] M. M. J. Treacy, T. W. Ebbesen, J. M. Gibson, *Nature* **1996**, *381*, 678–680.
[47] P. Poncharal, Z. L. Wang, D. Ugarte, W. A. de Heer, *Science* **1999**, *283*, 1513–1516.
[48] K. H. Liu, W. L. Wang, Z. Xu, L. Liao, X. D. Bai, E. G. Wang, *Appl. Phys. Lett.* **2006**, *89*, 221908–3.
[49] C.-Y. Nam, P. Jaroenapibal, D. Tham, D. E. Luzzi, S. Evoy, J. E. Fischer, *Nano Lett.* **2006**, *6*, 153–158.
[50] N. G. Chopra, A. Zettl, *Solid State Commun.* **1998**, *105*, 297–300.
[51] C. Q. Chen, Y. Shi, Y. S. Zhang, J. Zhu, Y. J. Yan, *Phys. Rev. Lett.* **2006**, *96*, 075505.
[52] H. Ohnishi, Y. Kondo, K. Takayanagi, *Nature* **1998**, *395*, 780–783.
[53] E. A. Stach, *Mater. Today* **2008**, *11*, 50–58.
[54] E. A. Stach, T. Freeman, A. M. Minor, D. K. Owen, J. Cummings, M. A. Wall, T. Chraska, R. Hull, J. W. Morris Jr., A. Zettl, U. Dahmen, *Microscopy Microanal.* **2001**, *7*, 507–517.
[55] Hysitron. *PI 95 TEM Picoindenter* July 25, 2011; Available from: http://www.hysitron.com/LinkClick.aspx?fileticket = 4kfuCAsVUNA%3d&tabid = 178.
[56] J. R. Greer, J. T. M. De Hosson, *Prog. Mater. Sci.* **2011**, *56*, 654–724.
[57] R. Agrawal, H. D. Espinosa, *J. Engin. Mater. Technology* **2009**, *131*, 041208.
[58] Z. W. Shan, R. K. Mishra, S. A. Syed Asif, O. L. Warren, A. M. Minor, *Nat. Mater.* **2008**, *7*, 115–119.
[59] J. Y. Huang, H. Zheng, S. X. Mao, Q. Li, G. T. Wang, *Nano Lett.* **2011**, *11*, 1618–1622.
[60] D. Kiener, A. M. Minor, *Nano Lett.* **2011**, *11*, 3816–3820.
[61] H. Guo, K. Chen, Y. Oh, K. Wang, C. Dejoie, S. A. S. Asif, O. L. Warren, Z. W. Shan, J. Wu, A. M. Minor, *Nano Lett.* **2011**, *11*, 3207–3213.
[62] J. Y. Huang, S. Chen, Z. Q. Wang, K. Kempa, Y. M. Wang, S. H. Jo, G. Chen, M. S. Dresselhaus, Z. F. Ren, *Nature* **2006**, *439*, 281–281.
[63] J. Y. Huang, S. Chen, S. H. Jo, Z. Wang, D. X. Han, G. Chen, M. S. Dresselhaus, Z. F. Ren, *Phys. Rev. Lett.* **2005**, *94*, 236802.
[64] K. Svensson, Y. Jompol, H. Olin, E. Olsson, *Rev. Scientific Instruments* **2003**, *74*, 4945–4947.
[65] Y. Naitoh, K. Takayanagi, M. Tomitori, *Surf. Sci.* **1996**, *357–358*, 208–212.
[66] Y. Liao, S. K. EswaraMoorthy, L. D. Marks, *Philosophical Magazine Lett.* **2010**, *90*, 219–223.
[67] D. Golberg, X. D. Bai, M. Mitome, C. C. Tang, C. Y. Zhi, Y. Bando, *Acta Materialia* **2007**, *55*, 1293–1298.
[68] D. Golberg, P. M. F. J. Costa, M. Mitome, Y. Bando, *J. Mater. Chem.* **2009**, *19*, 909–920.
[69] K. Jensen, W. Mickelson, A. Kis, A. Zettl, *Phys. Rev. B* **2007**, *76*, 195436.
[70] T. Kizuka, H. Ohmi, T. Sumi, K. Kumazawa, S. Deguchi, M. Naruse, S. Fujisawa, S. Sasaki, A. Yabe, Y. Enomoto, *Japanese J. Appl. Phys.* **2001**, *40*, L170.
[71] S. Fujisawa, T. Kikkawa, T. Kizuka, *Japanese J. Appl. Phys.* **2003**, *42*, L1433.
[72] T. Matsuda, T. Kizuka, *Japanese J. Appl. Phys.* **2009**, *48*, 115003.
[73] T. Kizuka, Y. Takatani, *Japanese J. Appl. Phys.* **2007**, *46*, 5706.
[74] T. Kizuka, Y. Takatani, K. Asaka, R. Yoshizaki, *Phys. Rev. B* **2005**, *72*, 035333.

[75] P. M. F. J. Costa, P. B. Cachim, U. K. Gautam, Y. Bando, D. Golberg, *Nanotechnology* **2009**, *20*, 405707.
[76] P. M. F. J. Costa, P. B. Cachim, U. K. Gautam, Y. Bando, D. Golberg, *Nanotechnology* **2009**, *20*, 405706.
[77] P. M. F. J. Costa, U. K. Gautam, M. Wang, Y. Bando, D. Golberg, *Carbon* **2009**, *47*, 541–544.
[78] A. Asthana, K.Momeni, A. Prasad, Y. K. Yap, R. S. Yassar, *Nanotechnology* **2011**, *22*, 265712.
[79] R. Agrawal, B. Peng, E. E. Gdoutos, H. D. Espinosa, *Nano Lett.* **2008**, *8*, 3668–3674.
[80] A. Nafari, D. Karlen, C. Rusu, K. Svensson, H. Olin, P. Enoksson, *J. Microelectromechanical Systems* **2008**, *17*, 328–333.
[81] Y. Zhu, H. D. Espinosa, *Proc. Natl. Acad. Sci. USA* **2005**, *102*, 14503–14508.
[82] R. Agrawal, B. Peng, H. D. Espinosa, *Nano Lett.* **2009**, *9*, 4177–4183.
[83] T. Filleter, R. Bernal, S. Li, H. D. Espinosa, *Adv. Mater.* **2011**, *23*, 2855–2860.
[84] T. Filleter, S. Ryu, K. Kang, J. Yin, R. A. Bernal, K. Sohn, S. Li, J. Huang, W. Cai, H. D. Espinosa, *Small*, **2012**, DOI:10.1002/smll.201200522.
[85] M. A. Haque, M. T. A. Saif, *Sens. Actuators A* **2002**, *97–98*, 239–245.
[86] M. Haque, M. Saif, *Experimental Mechanics* **2003**, *43*, 248–255.
[87] M. A. Haque, M. T. A. Saif, *J. Mater. Res.* **2005**, *20*, 1769–1777.
[88] M. A. Haque, H. D. Espinosa, H. J. Lee, *MRS Bull.* **2010**, *35*, 375.
[89] H. D. Espinosa, Y. Zhu, N. Moldovan, *J. Microelectromechanical Systems* **2007**, *16*, 1219–1231.
[90] Y. Zhu, A. Corigliano, H. D. Espinosa, *J. Micromechanics Microengineering* **2006**, *16*, 242–253.
[91] Y. Zhu, N. Moldovan, H. D. Espinosa, *Appl. Phys. Lett.* **2005**, *86*,
[92] M. Zhang, E. A. Olson, R. D. Twesten, J. G. Wen, L. H. Allen, I. M. Robertson, I. Petrov, *J. Mater. Res.* **2005**, *20*, 1802–1807.
[93] D. Zhang, J. M. Breguet, R. Clavel, V. Sivakov, S. Christiansen, J. Michler, *J. Microelectromechanical Systems* **2010**, *19*, 663–674.
[94] D. Zhang, J.-M. Breguet, R. Clavel, L. Philippe, I. Utke, J. Michler, *Nanotechnology* **2009**, *20*, 365706.
[95] D. Zhang, W. Drissen, J.-M. Breguet, R. Clavel, J. Michler, *J. Micromechanics Microengineering* **2009**, *19*, 075003.
[96] Y. Zhang, X. Liu, C. Ru, Y. L. Zhang, L. Dong, Y. Sun, *J. Microelectromechanical Systems* **2011**, *PP*, 1–9.
[97] M. Naraghi, T. Ozkan, I. Chasiotis, S. S. Hazra, M. P. de Boer, *J. Micromechanics Microengineering* **2010**, *20*, 125022.
[98] S. J. Eppell, B. N. Smith, H. Kahn, R. Ballarini, *J. Royal Society Interface* **2006**, *3*, 117–121.
[99] L. F. Allard, W. C. Bigelow, M. Jose-Yacaman, D. P. Nackashi, J. Damiano, S. E. Mick, *Microscopy Research and Technique* **2009**, *72*, 208–215.
[100] W. Kang, T. A. Saif, *MRS Communications* **2011**, *1*, 13–16.
[101] J. H. Han, M. T. A. Saif, *Review of Scientific Instruments* **2006**, *77*, 045102–8.
[102] H. D. Espinosa, R. A. Bernal, International Patent Application WO 2011/053346 A1
[103] X. D. Han, K. Zheng, Y. F. Zhang, X. N. Zhang, Z. Zhang, Z. L. Wang, *Adv. Mater.* **2007**, *19*, 2112–2118.
[104] S. Y. Xu, J. Xu, M. L. Tian, *Nanotechnology* **2006**, *17*, 1470.
[105] J. Cumings, A. Zettl, *Science* **2000**, *289*, 602–604.
[106] Z. L. Wang, P. Poncharal, W. A. d. Heer, *Pure Appl. Chem.* **2000**, *72*, 209–219.
[107] P. Jaroenapibal, D. E. Luzzi, S. Evoy, S. Arepalli, *Appl. Phys. Lett.* **2004**, *85*, 4328–4330.
[108] M. S. Wang, J. Y. Wang, Q. Chen, L. M. Peng, *Adv. Funct. Mater.* **2005**, *15*, 1825–1831.
[109] Z. Aslam, M. Abraham, A. Brown, B. Rand, R. Brydson, *J. Microscopy* **2008**, *231*, 144–155.
[110] D. Golberg, P. Costa, M. Mitome, Y. Bando, *Nano Res.* **2008**, *1*, 166–175.
[111] X. Bai, D. Golberg, Y. Bando, C. Zhi, C. Tang, M. Mitome, K. Kurashima, *Nano Lett.* **2007**, *7*, 632–637.
[112] P. M. F. J. Costa, X. Fang, S. Wang, Y. He, Y. Bando, M. Mitome, J. Zou, H. Huang, D. Golberg, *Microscopy Res. Technique* **2009**, *72*, 93–100.
[113] M. W. Larsson, L. R. Wallenberg, A. I. Persson, L. Samuelson, *Microscopy and Microanalysis* **2004**, *10*, 41–46.
[114] K. H. Liu, P. Gao, Z. Xu, X. D. Bai, E. G. Wang, *Appl. Phys. Lett.* **2008**, *92*, 213105–3.
[115] A. Asthana, K. Momeni, A. Prasad, Y. K. Yap, R. S. Yassar, *Appl. Phys. Lett.* **2009**, *95*, 172106–3.
[116] A. V. Desai, M. A. Haque, *Appl. Phys. Lett.* **2007**, *90*, 033102.
[117] D. Zhang, J. Breguet, R. Clavel, L. Philippe, I. Utke, J. Michler, *Nanotechnology* **2009**, *20*, 365706.
[118] A. Asthana, T. Shokuhfar, Q. Gao, P. Heiden, C. Friedrich, R. S. Yassar, *Appl. Phys. Lett.* **2010**, *97*, 072107–3.
[119] J. H. Luo, F. F. Wu, J. Y. Huang, J. Q. Wang, S. X. Mao, *Phys. Rev. Lett.* **2010**, *104*, 215503.
[120] N. W. Moore, J. Luo, J. Y. Huang, S. X. Mao, J. E. Houston, *Nano Lett.* **2009**, *9*, 2295–2299.
[121] Y. Lu, J. Y. Huang, C. Wang, S. Sun, J. Lou, *Nat. Nanotechnol.* **2010**, *5*, 218–224.
[122] S. Xu, M. Tian, J. Wang, J. Xu, J. M. Redwing, M. H. W. Chan, *Small* **2005**, *1*, 1221–1229.
[123] M. S. Wang, J. Y. Wang, Q. Chen, L. M. Peng, *Adv. Funct. Mater.* **2005**, *15*, 1825–1831.
[124] A. San Paulo, J. Bokor, R. T. Howe, R. He, P. Yang, D. Gao, C. Carraro, R. Maboudian, *Appl. Phys. Lett.* **2005**, *87*, 053111–3.
[125] Q. Jin, Y. L. Wang, T. Li, X. Li, F. F. Xu, *Science in China Series E* **2008**, *51*, 1491–1496.
[126] S. Gravier, M. Coulombier, A. Safi, N. Andre, A. Boe, J. P. Raskin, T. Pardoen, *J. Microelectromechanical Systems* **2009**, *18*, 555–569.
[127] M. Wang, I. Kaplan-Ashiri, X. Wei, R. Rosentsveig, H. Wagner, R. Tenne, L. Peng, *Nano Research* **2008**, *1*, 22–31.
[128] N. Agraït, A. L. Yeyati, J. M. van Ruitenbeek, *Physics Reports* **2003**, *377*, 81–279.
[129] A. Beche, J. L. Rouviere, L. Clement, J. M. Hartmann, *Appl. Phys. Lett.* **2009**, *95*, 123114–3.
[130] F. Liu, R. Collazo, S. Mita, Z. Sitar, S. J. Pennycook, G. Duscher, *Adv. Mater.* **2008**, *20*, 2162–2165.
[131] J. M. Vaughn, M. E. Kordesch, *J. Vacuum Sci. Technol. A* **2009**, *27*, 1058–1061.
[132] L.-C. Qin, *Reports on Progress in Physics* **2006**, *69*, 2761.
[133] K. J. Ganesh, M. Kawasaki, J. P. Zhou, P. J. Ferreira, *Microscopy and Microanalysis* **2010**, *16*, 614–621.
[134] K. J. Ganesh, A. D. Darbal, S. Rajasekhara, G. S. Rohrer, K. Barmak, P. J. Ferreira, *Nanotechnology* **2012**, 23
[135] G. Richter, K. Hillerich, D. S. Gianola, R. Moenig, O. Kraft, C. A. Volkert, *Nano Lett.* **2009**, *9*, 3048–3052.
[136] A. Kis, G. Csanyi, J. P. Salvetat, T. N. Lee, E. Couteau, A. J. Kulik, W. Benoit, J. Brugger, L. Forro, *Nat. Mater.* **2004**, *3*, 153–157.
[137] A. V. Krasheninnikov, F. Banhart, *Nat. Mater.* **2007**, *6*, 723–733.
[138] J. T. M. De Hosson, *Microscopy Research and Technique* **2009**, *72*, 250–260.
[139] *Nanofactory Instruments AB*. 26 July, 2011; Available from: http://www.nanofactory.com/Page.asp?nav = Nanomaterials&id = 1.
[140] P. Thibault, M. Dierolf, A. Menzel, O. Bunk, C. David, F. Pfeiffer, *Science* **2008**, *321*, 379–382.
[141] A technical account of the operation of the TEM or its application to a specific material system is beyond the scope if this review. Hence, the reader is referred to several specialized books about TEM, e.g., [14] and TEM of nanostructures e.g.,[15,16].

Received: February 13, 2012
Published online: August 20, 2012

